A p53-stabilizing agent, CP-31398, induces p21 expression with increased G2/M phase through the YY1 transcription factor in esophageal carcinoma and achieves synergistic growth suppressive effects in combination with an MDM2 or a FAK inhibitor on mesothelioma

（p53 蛋白を安定化する CP-31398 は、食道がんにおいて YY1 発現を抑制し p21 分子を誘導しＧ２/M 期を増加させるが、悪性中皮腫においては MDM2 あるいは FAK 阻害剤と相乗的な増殖抑制効果を示す）

千葉大学大学院医学薬学府

先端医学薬学専攻

（指導教授：田川雅敏）

鐘博雅

List of contents

Summary

Purpose: Restoration of p53 functions is one of the therapeutic strategies for cancer. CP-31398 was developed to stabilize conformation of p53 and increase p53 activity irrespective of the p53 genotype. We then investigated CP-31398-mediated effects on esophageal carcinoma with dysfunction in the p53 pathway, and mesothelioma with functional p53 pathway.

Methods: Human esophageal carcinoma and mesothelioma cells were treated with an agent and the cell viability was measured with a colorimetric WST assay. Cell cycle distributions were analyzed with a flow cytometry and expression of p53 and the relevant molecules was examined with Western blot analysis and RT-PCR. Cells were also treated with siRNA to knockdown the relevant molecular expression. Combinatory effects were analyzed with CalcySyn software.

Results and discussion: CP-31398 inhibited the cell growth in a *p53*-independent manner in esophageal carcinoma but in a *p53*-depedent way in mesothelioma. Increase of p53 levels were observed in most of *p53*-wild-type mesothelioma, while the levels decreased in *p53*-mutated mesothelioma and a majority of the esophageal carcinoma tested.

A combinatory use of CP-31398 and p53-stabilizing nutlin-3a produced synergistic growth suppressive effects in mesothelioma with the wild-type *p53* but to a lesser extent in those with mutated *p53* cells. The combination increased p53 levels and the phosphorylation, augmented cleavages of PARP and caspase-3 with increased sub-G1 populations, but decreased phosphorylated FAK levels. Defectinib, a FAK inhibitor, in combination with CP-31398, increased p53 levels and the phosphorylation together with dephosphorylation of FAK, and produced combinatory growth inhibitory effects in mesothelioma with the wild-type *p53* genotype.

In contrast, CP-31398 influenced expression of p53 and the downstream molecules in a cell-dependent manner in p53 dysfunctional esophageal carcinoma cells. Nevertheless, we found that all the cells increased p21 expression at the transcriptional level. Knockdown experiments with siRNA demonstrated that the CP-31398-mediated p21 up-regulation was unrelated with p53 levels but was associated with expression of YY1, a transcriptional factor which regulated p21 expression in a p53 relevant manner. We also showed that CP-31398-induced increase of G2/M populations was attributable to the up-regulated p21.

Conclusions: A combinatory use of a p53 stabilizing, CP-31398 and nutlin-3a, achieved synergistic cytotoxicity in part through p53-mediated down-regulation of FAK activity. Any combination of CP-31398, nutlin-3a and defactinib consequently could produce growth inhibitory effects in p53 wild-type cells. In contrast, CP-31398 augmented endogenous p21 levels and induced cell cycle changes in a p53-independent manner through down-regulation of YY1, a novel target of CP-31398.

Chapter 1: CP-31398-mediated effects on wild-type p53 tumors

1.1 Abstract

A majority of mesothelioma is defective of INK4A/ARF region, which consequently resulted in suppressed p53 expression and decreased the functions. We therefore examined a growth suppressive activity of CP-31398 which could restore the p53 functions irrespective of the p53 genotype and a possible combinatory suppressive action with nutlin-3a which augmented p53 levels with mesothelioma. CP-31398 inhibited the cell growth independently of the p53 genotype and increased p53 levels in most of p53-wild-type mesothelioma tested. Expression of p21, one of the p53 target molecules, also increased but in a p53 independent manner. In contrasts, nutlin-3a produced growth suppressive effects on mesothelioma with the wild-type p53 genotype and increased p53 levels in the cells. Moreover, nutlin-3a suppressed phosphorylation of focal adhesion kinase (FAK). A combinatory use of CP-31398 and nutlin-2a produced synergistic growth suppressive effects in mesothelioma with the p53 wild-type but to a less extent in those with mutated p53 cells. The combination inhibited the cell growth and increased sub-G1 populations. Western blot analysis indicated that the combination increased p53 levels and the phosphorylation, augmented cleavage of PARP and caspase-3, but decreased phosphorylated FAK levels. Defectinib, a FAK inhibitor, and CP-31398 increased p53 levels and the phosphorylation together with dephosphorylation of FAK and produced combinatory growth inhibitory effects. These data collectively suggested that combinatory effects of CP-31398 and nutlin-3a achieved apoptotic effects in part due to p53-mediated down-regulated FAK activity.

Keywords: mesothelioma, CP-31398, nutlin-3a, p53, FAK

1.2 Introduction

A majority of clinical specimens from mesothelioma patients showed deletion of INK4A and ARF regions with the *p53* genotype being wild-type (1). The deletion results in loss of the $p14^{ARF}$ and $p16^{INK4A}$ gene, and is consequently associated with an uninhibited activity of MDM2 which ubiquitinates p53 and promotes the degradation. Mesothelioma is therefore functionally defective of p53 activities despite bearing wild-type *p53* genotypes. Activation of the suppressed p53 functions can be one of the therapeutic strategies for mesothelioma patients who are currently treated with DNA damaging agents since p53 facilitates apoptotic cell death induced by the agents (2). Recent whole-exome sequencing data with the clinical specimens confirmed high frequency of the INK4A and ARF deletion and also revealed another common mutation at the *neurofibromatosis type 2* gene (*NF2*) (3, 4). The genetic mutation and aberrations downstream to NF2 resulted in a loss of functions in the Hippo pathway. The defective Hippo pathway influenced many aspects of biological functions, which included increased activity of focal adhesion kinase (FAK) (5). A relationship between expression of NF2 levels and NF2 mutation however remained unknown.

A small molecule targeting p53 is one of the therapeutic options for cancer. CP-31398 was initially designed to induce structural change of mutated p53 and to restore the functions (6, 7). Subsequent studies demonstrated that CP-31398 did not bind to p53 but augmented expression of wild-type p53 (8, 9). Previous studies also indicated that the agent was inhibitory to p53 ubiquitination (10) but the precise mechanism of augmenting p53 was not fully characterized. In contrast, nutlin-3a which blocked the

binding of MDM2 to p53 stabilized p53 expression through suppressing the ubiquitination (11). Both agents can increase endogenous p53 levels and contribute to cell death although the mechanism of up-regulating p53 is not always the same. CP-31398 was not examined for the growth suppressive activities with mesothelioma and nutlin-3a-mediated augmentation of p53 in mesothelioma was scarcely investigated (12). On the other hand, several FAK inhibitors were tested for anti-tumor effects in mesothelioma and produced cytotoxic effects on mesothelioma with decreased NF2 expression greater than on those with unimpaired expression (13). A FAK inhibitor was further investigated in a clinical study for the safety and feasibility (14).

Interactions between p53 and FAK were not well investigated, but enhanced FAK activity suppressed p53 expression in part due to inhibiting MDM2 functions (15, 16). FAK phosphorylated at tyrosine 397 was a marker for FAK activation and induced MDM2 phosphorylation, which subsequently facilitated ubiquitination of p53. In addition, FAK could be physically associated with p53 and block the transcription (17). In contrast, regulation of FAK activity by p53 was not reported, but a previous study showed that wild-type p53 but not mutated p53 down-regulated FAK transcripts probably through binding of p53 to the FAK regulatory region (18). These data suggested that enhanced p53 expression by CP-31398 or nutlin-3a was in part associated with down-regulated FAK activity.

In the present study, we examined growth suppressive activity of CP-31398 and nutlin-3a in mesothelioma with the wild-type or mutated *p53* genotype. The present study also investigated a combinatory role of both agents in the growth suppression and

a possible involvement of FAK inhibition to the combination effects.

1.3 Materials and Methods

Cells and agents

Human mesothelioma cell lines, MSTO-211H, NCI-H28, NCI-H226, NCI-H2052 and NCI-H2452, and mesothelial Met-5A cells which were immortalized with p53-inactivating SV40 T antigen, were purchased from American Type Culture Collection (Manassas, VA, USA). JMN-1B, EHMES-1 and EHMES-10 cells, established from Japanese patients, were kindly provided by Dr. Hironobu Hamada (Hiroshima University, Hiroshima, Japan) (19). MSTO-211H, NCI-H28, NCI-H226, NCI-H2052, EHMES-10 and NCI-H2452 cells had wild-type *p53* genotype but NCI-H2452 cells expressed truncated p53 protein (20). JMN-1B (G245S) and EHMES-1 (R273S) had mutated *p53* genotype. All the *p53* wild-type mesothelioma cells were defective of p14 and p16 expressions because of either loss of the transcription due to methylation in the regulatory regions or deletion of the genomic DNA. CP-31398, nutlin-3a and defactinib were purchased from Tocris Bioscience (Bristol, UK), ChemieTek (Indianapolis, IN, USA) and Selleck Chemicals (Houston, TX, USA), respectively.

In vitro cytotoxicity

Cells (2 x10^3/well) were seeded in 96-well plates and were treated with different concentrations of the agent. Cells were cultured for 4 days and the viability was determined with a colorimetric cell-counting WST kit (Wako, Osaka, Japan) (WST assay). The amount of formazan produced from WST-8 reagent was determined with the absorbance at 450 nm and the relative viability was calculated based on the

absorbance without any treatments. Combinatory effects and a half maximal inhibitory concentration (IC_{50}) values were estimated with CalcuSyn software (Biosoft, Cambridge, UK) based on the WST assay. Combination index (CI) values at respective fractions affected (Fa) points showed relative levels of suppressed cell viability. CI<1, CI=1 and CI>1 indicate synergistic, additive and antagonistic actions, respectively. Cell numbers were also counted with the trypan blue dye exclusion assay.

.

Cell cycle analysis

Cells treated with an agent for 2 days were fixed in ice-cold ethanol, incubated with RNase (50 μg/ml) and stained with propidium iodide (50 μg/ml). The staining profiles were analyzed with FACSCalibur (BD Biosciences, San Jose, CA, USA) and CellQuest software (BD Biosciences).

Western blot analysis

Cell lysate was subjected to sodium dodecyl sulfate polyacrylamide gel electrophoresis, transferred to a nylon filter and then reacted with antibody against phosphorylated p53 at Ser 15 (catalog number:#9284) or 46 (#2521), p21 (#2947), caspase-3 (#9668), cleaved caspase-3 (#9661), cleaved caspase-8 (#9496), cleaved caspase-9 (#9505), PARP (which also detects cleaved PARP) (#4108), FAK (#3285), phosphorylated FAK at Tyr397 (#3283), AMPKα (#2532), phosphorylated AMPKα (Thr172) (#2535) (Cell Signaling, Danvers, MA, USA), p53 (Ab-6, Clone DO-1) (Thermo Fisher Scientific, Fremont, CA, USA), MDM2 (sc-965, Santa Cruz Biotechnology, Santa Cruz, CA,

USA) and actin (#4970) (Cell Signaling) as a loading control followed by appropriate second antibody. The membranes were incubated with the ECL system (GE Healthcare, Buckinghamshire, UK) and imaged with ImageQuant LAS 4000 (GE Healthcare).

Statistical analysis

ANOVA test was used to statistically analyze data.

1.4 Results

Growth inhibitory effects of CP-31398

We examined CP-31398-mediated growth inhibition with human mesothelioma with wild-type and mutated *p53* genotypes (Figure 1A). We classified NCI-H2452 and Met-5A cells as a p53-mutated group since NCI-H2452 cells expressed truncated p53 protein (20) and Met-5A expressed SV40 T antigen. A colorimetric assay with the WST reagent showed that CP-31398 produced the inhibitory effects on mesothelioma and the IC_{50} values were not different among the cells with regard to the *p53* genotype (average IC_{50} value $\pm$ SE: 7.51 $\pm$ 1.06 μM for cells with the wild-type *p53*, 5.57 $\pm$ 0.11 for those with mutated p53 group) (P=0.15). We also tested the growth inhibitory effects with a dye exclusion assay (Figure 1B). Cells treated with CP-31398 at 3 μM showed growth retardation and those treated with a higher concentration decreased cell numbers. These data indicated that CP-31398 produced anti-tumor effects on mesothelioma irrespective of the *p53* genotype.

Increased endogenous p53 expression with CP-31398

We then examined whether CP-31398 augmented expression levels of p53 (Figure 1C). CP-31398-treated cells with the wild-type *p53* genotype increased the p53 levels except EHMES-10 cells, whereas the p53-mutated group showed inconsistent results. NCI-H2542 cells showed decreased p53 of a truncated form, JMN-1B cells expressed the molecules at 53 kDa and a lower size, EHMES-1 cells up-regulated the expression, and Met-5A cells remained unchanged for the expression. Expression of p21, one of the p53

targets with an apoptosis-inhibitory function, was temporally up-regulated in mesothelioma with wild-type *p53* and NCI-H2452, whereas the p53-mutated cells rather down-regulated the p21 levels. A previous study showed that CP-31398 could activate the AMP-activated protein kinase (AMPK) pathway through up-regulated phosphorylation of AMPK (21), but the current study showed rather down-regulation of AMPK or phosphorylated AMPK except NCI-H2052 and EHMES-10 cells. These data collective indicated that CP-31398 could augment p53 levels in mesothelioma with the wild-type *p53* but the growth suppressive effects was not linked with the p53 up-regulation.

Growth inhibitory effects of nutlin-3a

We also examined nutlin-3a-mediated growth inhibition in mesothelioma with the colorimetric assay (Figure 2A). Sensitivity to nutlin-3a was greater in cells of the wild-type *p53* excluding EHMES-10 cells (average IC_{50} $\pm$ SE: 3.64 $\pm$ 2.87 μM) than in those of the p53-mutated group (30.49 $\pm$ 7.93) ($P<0.01$). A mechanism of resistance to nultin-3a in EHMES-10 remained uncharacterized but they expressed MDM2 at a low level similarly to mutated *p53*-bearing cells (data not shown). We then examined p53 expression in representative mesothelioma cells after nutlin-3a treatments (Figure 2B). Mesothelioma with the wild-type *p53* up-regulated p53 and the phosphorylation at Ser 15, whereas those of mutated *p53* to a less extent augmented p53 and the phosphorylation. We also examined expression levels of FAK and phosphorylated FAK at Tyr 397 and found that nultin-3a suppressed the phosphorylated expression except

NCI-H28 and EHMES-1 cells although FAK levels were unchanged except JMN-1B cells. The nutlin-3a-mediated down-regulation of phosphorylated FAK was therefore not linked with the *p53* genotype.

Combination of CP-31398 and nutlin-3a produced synergistic growth inhibition in the *p53* wild-type cells

We next examined combinatory effects of CP-31398 and nutlin-3a on mesothelioma with the wild-type and mutated *p53* (Figure 3). The relative growth of mesothelioma with the wild-type *p53* was suppressed in the combination and the CI values showed that the combination achieved synergistic effects (Figure 3A). In contrast, mesothelioma with mutated *p53* required a high concentration of nutlin-3a for growth suppression. The CI values consequently did not show synergistic but rather antagonistic in a majority of Fa points although relative viability tested with WST assay was not much different from that in NCI-H28 cells. We also counted live cell numbers of mesothelioma with the wild-type *p53* and showed that the combinatory use of CP-31398 and nutlin-3a suppressed the cell growth greater than a treatment with the single agent (Figure 3B). We then tested cell cycle progression after the treatments (Figure 3C). CP-31398 increased S-phase and G2/M-phase populations, and the combination augmented sub-G1 populations in MSTO-211H cells (Figure 3C, Table 1). In contrast, the combination in NCI-H28 cells did not increase sub-G1 fractions although CP-31398 augmented G2/M-phase and nutlin-3a slightly enhanced sub-G1 populations. These data suggested that the combination induced cell death in MSTO-211H cells and cell

cycle arrest in NCI-H28 cells.

Combination of CP-31398 and nultin-3a increased p53 levels and suppressed FAK phosphorylation

We investigated a molecular mechanism of the growth inhibition in MSTO-211H and NCI-H28 cells with Western blot analysis (Figure 4). The combination of CP-31398 and nutlin-3a increased p53 and the phosphorylation levels greater than a treatment with either CP-31398 or nutlin-3a. Levels of p21 and MDM2, p53 target molecules, were consequently up-regulated in the combination. Expression of caspase-3 increased in both cells treated with nutlin-3a and the combination, and cleavage of caspase-3 was detected in the combination. Caspase-8 and -9 were cleaved in MSTO-211H treated with the combination but not in NCI-H28 cells. PARP cleavages increased in CP-31398- and the combination-treated MSTO-211H cells, and to a less extent in the combination-treated NCI-H28 cells. These data collectively indicated that the combination activated the p53 pathway in both cells but apoptosis induction was greater in MSTO-211H than in NCI-H28 cells. In addition, we found that phosphorylation of FAK was down-regulated in CP-31398-treated and combination-treated cells compared with corresponding total FAK levels on both cell lines. Meanwhile, MSTO-211H but not NCI-H28 cells decreased the phosphorylation with nutlin-3a as described above (Figure 2B). These data also suggested that decreased FAK activity contributed to the combination-induced growth inhibitory effects.

Inhibition of FAK augmented CP-31398-mediated growth effects

We examined a possible contribution of FAK inhibition to the growth suppression induced by the combinatory use of CP-31398 and nutlin-3a. Defactinib was a FAK inhibitor and was examined in combination with CP-31398 for the growth inhibitory effects in MSTO-211H and NCI-H28 cells (Figure 5A). The combination produced synergistic effects in both cells. We also investigated molecular events induced by the combination with Western blot analysis (Figure 5B). A combinatory use of CP-31398 and defectinib augmented p53 and the phosphorylation levels in comparison with a single agent. CP-31398 and defectinib inhibited FAK phosphorylation and the combination kept the phosphorylation at a low level despite constant expression of FAK. These data indicated that FAK inhibition produced growth suppressive effects with CP-31398 and suggested that the combinatory effects achieved by CP-31398 and nutlin-3a were partly attributable to the FAK inhibition.

1.5 Discussion

We demonstrated in the present study that CP-31398 augmented endogenous p53 levels and a combinatory use with nutlin-3a achieved synergistic growth inhibitory effects in mesothelioma with wild-type *p53* genotypes. Moreover, nutlin-3a which increased endogenous p53 expression down-regulated FAK phosphorylation and combination of CP-31398 and a FAK inhibitor achieved growth suppression. The current study firstly reported to our knowledge anti-tumor effects of CP-31398 in mesothelioma and combinatory growth suppression with CP-31398 and an MDM2 inhibitor.

CP-31398 was initially study as an agent to convert mutated p53 to wild-type p53 but the precise mechanism of CP-31398 to restore p53 functions in cells with mutated *p53* genotype was not well characterized (22, 23). The present study showed that CP-31398-mediate changes of p53 expression in p53-mutated mesothelioma were inconsistent and CP-31398 increased p53 levels in most of the mesothelioma with the wild-type *p53*. Furthermore, the growth suppressive activity was irrelevant to *p53* genotype. In contrast, p21 expression was augmented with a low concentration of CP-31398 in the *p53* wild-type cells and was down-regulated in the p53-mutated group except NCI-H2452 cells. The p21 response was not concordant to p53 up-regulation as found in EHMES-10 and NCI-H2452 cells which showed p21 up-regulation even under p53 down-regulation. Expression of p21 in CP-31398-treated cells was thus not solely regulated by p53 and the p21 induction was independent of *p53* genotype. Previous study also reported that p21 augmentation by CP-31398 was irrelevant to p53 but the mechanism of p21 up-regulation remained uncharacterized (9, 24). On the other hand,

p21 was induced with non-p53 pathways (25, 26) and functioned as an inhibitor for apoptosis (27). We observed down-regulated p21 at a high concentration of CP-31398, which could account for cell death induction by CP-31398. Nutlin-3a also augmented p21 expression even in p53-muated cells, and the p21-enhancing mechanism was consequently different between CP-31398 and nutlin-3a although both agents induced p21 in a p53-independent manner.

A combinatory use of CP-31398 and nutlin-3a achieved synergistic growth suppressive effects in mesothelioma with the wild-type *p53* genotype. We demonstrated increased sub-G1 fractions in MSTO-211H cells and cleavage of caspase-8, caspase-3, PARP and to a less extent caspase-9 in the combination. Induction of the apoptotic cascade was correlated with increased p53 and the phosphorylation levels. On the other hand, NCI-H28 cells did not show increased sub-G1 fractions although live cell numbers were slightly decreased in the combination. We detected increased p53 and the phosphorylation in the combination but cleavages of PARP and caspase-3 were minimal. Moreover, caspase-8 and caspase-9 were scarcely cleaved. These data showed that the combination in NCI-H28 cells induced cell cycle arrest due to increased p53 levels. The combinatory effects were not significant in cells with mutated *p53* compared with in those bearing the wild-type *p53*. We needed to use nultin-3a at a higher concentration in EHMS-1 and JMN-1B cells than in the wild-type *p53* cells to detect combinatory effects since the mutated cells were resistant to nutlin-3a-mediated growth suppressive effects. The differential CI values between the wild-type cells and mutated cells were attributable to distinct nutlin-3a concentrations used although the profiles

with colorimetric assay looked similar each other. We presume that the combinatory effects was subjected to how p53 elevation-mediated growth inhibition was achieved by nultin-3a. A low concentration of nutlin-3a augmented p53 in the wild-type cells and further enhanced p53 levels by CP-31398 favored cell death and cell cycle arrest.

FAK play a certain role in regulation of p53 expression through MDM2 and decreased FAK with the sh-RNA augmented p53 levels through down-regulated MDM2 (15, 16). The present study also showed that defactinib decreased FAK phosphorylation and increased p53 in NCI-H28 and MSTO-211H cells. Furthermore, CP-31398 suppressed FAK phosphorylation in both cells. A combinatory use of defactinib and CP-31398 consequently augmented p53 levels and the phosphorylation, and kept FAK phosphorylation down-regulated. These data indicated that inhibition of FAK activity led to p53 elevation and further suggested that p53 up-regulation reversely down-regulated FAK activity. In contrast to FAK inhibition-mediated p53 regulation, p53-induced FAK dephosphorylation was not yet reported. A mechanism of p53-induced FAK down-regulation was due to the p53 binding to a regulatory region of *FAK* gene and subsequent inhibition of the p53 transcripts (18). The preset study however showed that FAK phosphorylation but not FAK expression was down-regulated by augmented p53, indicating that p53 blocked FAK-mediated signaling. The mechanism of p53-mediated downregulation of FAK phosphorylation remained unknown, but it may be linked with p53-mediated cell growth inhibition. Expression of p53 retarded cell growth and came to shut off a growth signal from extracellular matrix, which can dissociate FAK from cell membrane to be dephosphorylated. The down-regulation of

FAK phosphorylation was nevertheless irrelevant to *p53* genotype. Furthermore, MSTO-211H cells treated with nutlin-3a decreased FAK phosphorylation but NCI-H28 cells did not although both cells increased p53 by nutlin-3a. The down-regulation of FAK phosphorylation caused not only by nutlin-3a but also by CP-31398 can therefore be mediated partly with non-p53 pathways besides the p53 pathway. The colorimetric assay however showed that defactinib and CP-31398 achieved combinatory effects in accordance with augmented p53 and down-regulated FAK phosphorylation. These data collectively suggested that the combinatory effects in wild-type *p53* cells were in part linked with augmenting p53 and down-regulating FAK actions, and also implied that combinatory effects with nultin-3a and CP-31398 were mediated to some extent thorough inhibition of FAK activity.

In the present study, we firstly reported to our knowledge that CP-31398 produced combinatory growth suppressive effects with nutlin-3a and the effects could be achieved through FAK inhibition. In addition, nutlin-3a and CP-31398 decreased FAK phosphorylation without influencing FAK expression. A FAK inhibitor is a potentially therapeutic agent for mesothelioma since the *NF2* mutation, commonly found in mesothelioma specimens, was linked with augmented FAK. An MDM2 inhibitor augmented endogenous wild-type p53 levels, which is one of the common features in mesothelioma, and consequently contributed to cell growth inhibition. The current study thus suggested that these three agents, in any of the combinations, are candidates for a therapeutic option for mesothelioma.

Chapter 2: CP-31398-mediated effects on p53 dysfunctional tumors

2.1 Abstract

Restoration of p53 functions is one of the therapeutic strategies for esophageal carcinoma which is often defective of the p53 pathway. We examined effects of CP-31398 which potentially increased expression of wild-type p53 or converted mutated p53 to the wild-type. We used 9 kinds of human squamous esophageal carcinoma cells with different *p53* genotypes and examined expression of p53 and the related molecules in CP-31398-treated cells. Cisplatin induced cleavages of PARP and caspase-3 without increase of p53 levels, indicating that the p53 down-stream pathway was disrupted in these cells. CP-31398 induced growth retardation but the cytotoxic effects were irrelevant to *p53* genotype. CP-31398 influenced expression of p53 and the downstream molecules in a cell-dependent manner, but constantly increased p21 expression at the transcriptional level with decreased YY1 expression. Knockdown experiments with siRNA demonstrated that the CP-31398-mediated p21 up-regulation was unrelated with p53 expression but was associated with YY1 expression. We also showed that CP-31398-induced increase of G2/M populations was attributable to the up-regulated p21. These data collectively indicate that CP-31398 augmented endogenous p21 levels and induced cell cycle changes in a p53-independent manner but through regulation of YY1, which is a novel target of CP-31398.

Keywords CP-31398; esophageal carcinoma; p53; p21; YY1; G2/M arrest

2.2 Introduction

An advanced case of esophageal carcinoma remains intractable because of the frequent invasion into vital organs in the vicinity (28). A combination of chemotherapy and radiation is applicable to the patients and they can be subjected to surgical procedures thereafter. The current chemotherapeutic agents for esophageal carcinoma are primarily DNA-damaging agents such as cisplatin (CDDP) and DNA synthesis inhibitors. Recent genome-wide sequencing data however demonstrated that the major genetic abnormality was associated with gene mutations in the p53 pathway, which resulted in p53 dysfunction and consequently in resistance to the DNA damaging anti-cancer agents (29, 30). Reconstitution of the authentic p53 pathway is therefore one of strategies for esophageal carcinoma to enhance anti-tumor effects by the chemotherapeutic agents.

A number of agents acting on p53 expression levels are now being investigated for the therapeutic efficacy and some of them have been examined for the possible clinical feasibility (31). An agent to inhibit a binding between p53 and MDM2 molecules which ubiquitinate and degrade p53 is a candidate to increase p53 stability (23). An MDM2 inhibitor can increase p53 levels but the effectiveness is restricted only in cells with the wild-type *p53* genotype. A different type of an agent is needed to activate the p53 pathway in cells with mutated *p53* genotype. CP31398 and PRIMA-1 belong to a functionally different group from MDM2 inhibitors and augment or activate the p53 downstream pathway irrespective of the *p53* genotypes (6, 32). The agents can not only increase expression of the wild-type p53 also convert specific mutated p53 such as

codon 248, 249 and 273 to the wild-type (10). Nevertheless, the agents with the p53-converting activity or MDM2 inhibitors have not yet examined for the cytotoxicity in esophageal carcinoma except a report dealing with nutlin-3a, one of the MDM2 inhibitors (33).

We previously showed that adenoviruses expressing the wild-type p53 (Ad-p53) induced cell death in esophageal carcinoma and increased susceptibility to chemotherapeutic agents (34). These data suggested that activation of the p53 pathway with exogenously expressed p53 was another therapeutic strategy for esophageal carcinoma despite the whole exome sequencing data which indicated that a majority of esophageal carcinoma was defective of the p53 pathway(29, 30). We further conducted a clinical study to intratumorally administer Ad-p53 into esophageal carcinoma and demonstrated the safety and clinical efficacy (35). These data collectively suggested that stimulation of the p53 pathway with transduced p53 or up-regulated endogenous p53 produced cytotoxic effects on esophageal carcinoma and indicated that restoration of the p53 pathway played an important role in the treatment.

In the present study, we investigated a possible therapeutic efficacy of CP-31398, an agent capable to convert mutated p53 into the wild-type and to augment wild-type p53 level. We analyzed how 9 kinds of esophageal carcinoma cells responded to a DNA damaging agent in terms of the p53 pathway and examined whether CP-31398 activated the p53 pathway in the esophageal carcinoma cells. The present study also analyzed a mechanism of CP-31398-mediated induction of p21 in a p53-independent manner.

2.3 Materials and methods

Cells and agents

Human esophageal squamous cell carcinoma, TE-1 (mutated *p53*; at codon 272 Val to Met), TE-2 (wild-type *p53*), TE-10 (mutated at 242 Cys to Tyr), TE-11 (wild-type), YES-2 (mutated at 236 Tyr to Asn), YES-4 (wild-type), YES-5 (mutated at 280 Arg to Gly), YES-6 (wild-type) and T.Tn (mutated at 214 His to Arg and at 258 Glu to stop) cells, were from Cell Resource Center for Biomedical Research, Tohoku University (Sendai, Japan). Human mesothelioma, MSTO-211H (wild-type) and NCI-H28 (wild-type) cells, were purchased from American Type Culture Collection (Manassas, VA, USA), and JMN-1B (mutated) and EHMES-1 (mutated) which were established from Japanese patients, were kindly provided by Dr. Hironobu Hamada (Hiroshima University, Hiroshima, Japan) (19). All cells were cultured with RPMI-1640 medium supplemented with 10% fetal calf serum. CP-31398 and nutlin-3a were purchased from Tocris Bioscience (Bristol, UK), and ChemieTek (Indianapolis, IN, USA), respectively.

In vitro cytotoxicity and cell proliferation

Cells (2 x10^3/well) were seeded in 96-well plates and were cultured for 4 days with different concentrations of an agent. Cell viability was determined with a cell-counting WST kit (Wako, Osaka, Japan) (WST assay). The amount of formazan produced from a WST-a reagent was determined with the absorbance at 450 nm and the relative viability was calculated based on the absorbance without any treatments. Live cell numbers were also counted with the trypan blue dye (dye exclusion assay). Half

maximal inhibitory concentration (IC_{50}) values were also estimated with the CalcuSyn software (Biosoft, Cambridge, UK).

Western blot analysis

Cell lysate was subjected to sodium dodecyl sulfate polyacrylamide gel electrophoresis. The protein was transferred to a nylon filter and was hybridized with antibody against phosphorylated p53 at Ser 15 (catalog number:#9284) or 46 (#2521), p21 (#2947), caspase-3 (#9668), cleaved caspase-3 (#9661), poly ADP ribose polymerase (PARP) (which also detected cleaved PARP) (#4108), AMPKα (#2532), phosphorylated AMPKα (Thr172) (#2535), 4E-BP1 (#9452), phosphorylated 4E-BP1 (Thr37/46) (#9459), p70S6K (#9202), phosphorylated p70S6K (Thr389) (#9205) (Cell Signaling, Danvers, MA, USA), p53 (Ab-6, Clone DO-1) (#MS-187-P0), phosphorylated p21 (Thr145) (#PA5-36677) (Thermo Fisher Scientific, Fremont, CA, USA), MDM2 (sc-965), YY1 (sc-7341) (Santa Cruz Biotechnology, Santa Cruz, CA, USA), p63 (ab735), p73 (ab40658), YY2 (ab116507) (Abcam, Cambridge, UK), γ-H2AX (#613401, BioLegend, San Diego, CA, USA), Kip1/p27 (#610241) (BD biosciences, San Jose, CA, USA) and actin (#4970) (Cell Signaling) as a loading control followed by appropriate second antibody. The membranes were developed with the ECL system (GE Healthcare, Buckinghamshire, UK) and imaged with ImageQuant LAS 4000 (GE Healthcare).

RNA interference

Cells were transfected with small interfering RNA (siRNA) duplex targeting YY1 (#sc-36863), p21 (#sc-29427) (Santa Cruz Biotechnology, Santa Cruz, CA, USA), p53(#TP53-VHS40367) or with non-coding siRNA(#12935-114) as a control (Thermo Fisher Scientific, Fremont, CA, USA) using Lipofectamine RNAiMAX according to the manufacturer's protocol (Thermo Fisher Scientific).

Cell cycle analysis

Cells treated with an agent were fixed in ice-cold 100% ethanol, incubated with RNase (50 μg/ml) and stained with propidium iodide (50 μg/ml). The staining profiles were analyzed with FACSCalibur (BD Biosciences, San Jose, CA, USA) and CellQuest software (BD Biosciences).

Reverse transcription-polymerase chain reaction (RT-PCR)

First-strand cDNA was synthesized with Superscript III reverse transcriptase (Invitrogen, Carlsbad, CA) and amplification of equal amounts of the cDNA was performed with the following primers and conditions: for the p53 gene, 5'-CTGCCCTCAACAAGATGTTTTG-3' (sense) and 5'-CTATCTGAGCAGCGCTCATGG-3' (anti-sense), and 30 sec at 96 ℃ for denature/90 sec at 65 ℃ for annealing/36 cycles; for the p21 gene, 5'-GACACCACTGGAGGGTGACT-3' (sense) and 5'-GGCGTTTGGAGTGGTAGAAA-3' (anti-sense), and 10 sec at 94 ℃/20 sec at 48 ℃/35 cycles; for the glyceraldehyde-3-phosphate dehydrogenase (GAPDH) gene, 5'-

ACCACAGTCCATGCCATCAC-3’ (sense) and 5’-TCCACCACCCTGTTGCTGTA-3’ (anti-sense), and 15 sec at 94 ℃/15 sec at 60 ℃/30 cycles. The products were analyzed with gel electrophoresis.

2.4 Results

Esophageal carcinoma cells were defective of p53 activation

We examined possible activation of p53-mediated pathway with CDDP, a DNA damaging agent, in 9 kinds of human esophageal squamous cell carcinoma with different *p53* genotype (Figure 6). TE-11 and YES-4 cells, with wild-type *p53* genotype, temporally increased p53 levels and the phosphorylation at serine 15 after CDDP treatments, while the other p53 wild-type cells, TE-2 and YES-6 cells, hardly expressed p53 and did not increase the expression (Figure 6A). We also found that CDDP treatments scarcely increased p53 transcripts (Figure 6B), indicating that the p53 increase in TE-11 and YES-4 cells were due to a posttranscriptional regulation. Expression of p21, a target of p53 activation, was rather down-regulated in TE-11, YES-4 and to a lesser extent in YES-6 cells, but slightly increased in TE-2 cells. Expression of p73, belonging to the p53 family proteins, was variable among the cells in both form, TAp73α and deltaNp73, and p63 levels were suppressed by CDDP treatments. Induction of the DNA damage was evidenced by up-regulated γ-H2AX expression and all the cells showed cleavages of caspase-3 and PARP. These data collectively indicated that CDDP induced cell death without activation of p53 and the other p53 family proteins, and suggested that the p53 downstream pathway was non-functional in esophageal carcinoma despite the wild-type *p53* genotype.

Esophageal carcinoma cells with mutated *p53* genotypes showed differential expression levels of p53 and the phosphorylation after CDDP treatments (Figure 6C). TE-1 and TE-10 cells decreased p53 and the phosphorylation levels, whereas YES-2

and T.Tn cells increased both p53 levels and YES-5 cells did not influence the levels. Expression levels of p21 and p63 were down-regulated except p21 in YES-2 cells, but those of TAp73α and deltaNp73 remained unchanged except TAp73α in TE-1. CDDP-treated cells showed increased γ-H2AX and cleavages of PARP and caspase-3 in these cells. These data therefore indicated that a DNA damaging agent activated apoptotic pathway in a p53-independent manner in esophageal carcinoma cells.

We also examined whether the p53 downstream pathway in the esophageal carcinoma cells functioned with relative sensitivity to nutlin-3a (Figure 6D). Nutlin-3a, an inhibitor for interaction between MDM2 and p53, induced growth inhibition in cells with the wild-type *p53* genotype, whereas cells with mutated *p53* genotype were insensitive to nutlin-3a (36). We used mesothelioma cells with the wild-type and with mutated *p53* genotype and showed that those with the wild-type *p53* were subjected to growth inhibition and sensitive to nutlin-3a (average $IC_{50} \pm$ SE: 3.77 ± 1.71), whereas those with mutated *p53* were insensitive (33.92 ± 2.94) (Figure 6E). We then tested sensitivity of esophageal carcinoma cells to nutlin-3a and showed that the IC50 values were all similar to that of mesothelioma with mutated *p53* and the sensitivity was not influenced by the *p53* genotype. These data collectively indicated that the p53 downstream pathway in esophageal carcinoma were non-functional irrespective of the *p53* genotype and suggested that the cell death by DNA damage was irrelevant to the p53 pathways.

Growth suppression produced by CP-31398 was irrelevant to the p53 genotype

We then examined growth suppressive activity of CP-31398 with the esophageal carcinoma (Figure 7A). Sensitivity of cells with the wild-type *p53* to CP-31398 (IC_{50}=4.97 ± 1.23) was not different from that of cells with mutated *p53* (4.27 ± 0.40), indicating that the susceptibility was not associated with the *p53* genotype (P=0.26). We also tested susceptibility of mesothelioma to CP-31398 and found that CP-31398 inhibited the cell growth in a p53-independent manner (wild-type p53: 6.80 ± 2.12, mutated p53: 5.55 ± 0.20) (Figure 7B). We examined live cell numbers of esophageal carcinoma cells treated with CP-31398 (Figure 7C). CP-31398 treatments induced growth retardation and decreased live cell numbers, indicating that CP-31398 produced cytostatic and cytotoxic effects depending on the agent dose and the effects was not associated with the *p53* genotype. These data collective indicated that mechanism of CD-31398-mediated cytotoxicity was irrelevant to the p53 pathway.

Cell cycle progression by CP-31398

We tested cell cycle progression of cells treated with CP-31398 (Figure 7D, Table 2). We found that a small percentage of TE-1, TE-2 and YES-5 cells showed an over-4N population (hyperploidy), and TE-4 and TE-11 cells constantly had a sub-G1 population which was different from a cell death-liked sub-G fraction. The hyperploidy fractions and the persistent sub-G1 population could be attributable to an abnormal cell division process and nucleoli, respectively, all of which were probably pertinent to malignant transformation. CP-31398-treated cells showed increased G2/M populations in all the cells tested (Figure 7E), hyperploidy fractions in TE-2, TE-10, YES-2 and T.Tn cells,

and sub-G populations in YES-2, YES-5, YES-6 and T.Tn cells.

Expression of p53 and the relevant molecules induced by CP-31398

We investigated expression of p53 and the relevant molecules in esophageal carcinoma cells treated with CP-31398 (Figure 8). CP-31398 increased p53 expression in TE-10 cells but decreased the levels in TE-1, YES-2 and YES-5 cells. The phosphorylated p53 levels at Ser 15 in TE-10 and YES-2 cells matched with the respective changes of p53 expression, but those at Ser 46 in these cells were not associated with the p53 changes. TE-1 cells showed no change of the phosphorylated p53 levels and YES-5 cells decreased only Ser 46 phosphorylation. T.Tn cells up-regulated p53 phosphorylation in both Ser 15 and 46 but the p53 levels remained the same, and TE-11 cells increased the phosphorylation at Ser 15 but decreased at Ser 46 with constant p53 levels. Expression of p53 and the phosphorylation remained unchanged in YES-4, but TE-2 and YES-6 scarcely expressed p53 and the phosphorylation at Ser 15 as shown in CDDP-treated cells. CP-31398 did not increase p53 levels not only in *p53* wild-type cells but in mutated *p53* cells, suggesting that CP-31398 did not increase stability of wild-type p53 or conversion from mutated p53 to the wild-type p53. As for other p53 family proteins, esophageal carcinoma cells decreased p63 and/or p73 isoform expression levels except TE-1 and TE-10 cells, and consequently CP-31398-mediated changes of the p53 family proteins were not linked with the p53 genotypes. Expression of MDM2, a target of the p53 pathway, was constant except in TE-2 and YES-4 cells which down-regulated the expression, whereas expression of p21, also the p53 target molecules, was up-regulated

in all the cells. Phosphorylated p21 at Thr 145, a marker of p21 stability, was however not correlated with increased p21 levels, suggesting that augmented p21 expression was attributable to the transcriptional activation. CP-31398-induced changes of p27 expression were variable among the cells and the expressional changes were inconsistent with the p53 changes. Increased cleavage of PARP or caspase-3 was detected in all the cells except TE-2 cells, indicating that CP-31398 induced the apoptotic pathway in a p53-independent manner.

We also examined expression of YY2, p53-bindindg molecules involved in p21 transcriptional activation (37), and that of AMPK which was in an upstream pathway of 4E-BP1 which played a role in p21 stability (25). Expression of YY2 increased in TE-10 and to a lesser extent in TE-11 cells, but decreased in YES-2 cells. Other cells treated with CP-31398 did not show any changes of YY2 expression. Expression of AMPK or the phosphorylation was down-regulated in the majority of cells, but TE-11 and YES-2 cells increased the phosphorylation levels. YES-4 cells was not influenced in both expression levels and YES-5 minimally increased AMPK expression. Expression levels of 4E-BP1, p70S6K and respective phosphorylated molecules was in general down-regulated with CP-31398 except increased levels of phosphorylated 4E-BP1 and p70S6K in YES-4, marginally increased p70S6K in YES-6 and 4E-BP1 in T.Tn cells. These data collectively indicated that YY2 or 4E-BP1 expression profiles did not matched with the p21 up-regulation by CP-31398 and suggested that both molecules were not responsible for the augmented expression.

We further examined expression of p53 and the related molecules in CP-31398-

treated cells with different doses and incubation periods (Figure 9). Expression of p53 was down-regulated in the majority in dose- and time-dependent manners except TE-10 which increased the level, T.Tn with unchanged levels, TE-2 and TE-6 which did not expressed p53. The responses to CP-31398 in respective cells were thus different from those to CDDP, indicating that CP-31398 did not induce the same DNA damage as CDDP did. The dose and time course experiments showed that expression of p21 was up-regulated with CP-31398 compared with the expression in untreated cells. Expression of YY1, a transcriptional factor which negatively regulates p21 transcripts (38, 39), decreased with CP-31398 treatments except TE-10 cells that increased the level. These data collectively suggested that CP-31398-mediated p21 increase was independent of the p53 pathway and was well associated with YY1 expression.

CP-31398 activated p21 transcription and YY1 involvement in the p21 induction

We investigated whether the CP-31398 regulated p21 expression at the transcriptional level with RT-PCR (Figure 10A). An amount of p21 transcripts increased in esophageal carcinoma cells treated with CP-31398 and the up-regulation was dependent on CP-31398 concentrations. All the esophageal carcinoma showed increase of p21 transcripts but the mRNA expression levels were not matched with the protein levels, suggesting that p21 expression was also regulated at the post-transcriptional level.

We examined a possible involvement of p53 in the CP-31398-mediated p21 up-regulation with siRNA in 4 representative cells regarding *p53* genotype. (Figure 10B). Expression of p53 was down-regulated with p53-siRNA but not with control siRNA

irrespective of the genotype. Knockdown of p53 scarcely influenced endogenous p21 expression or the CP-31398-induced augmented p21 levels. Cells treated with control siRNA augmented p21 expression after CP-31398 treatments. These data with the siRNA indicated that the CP-mediated p21 augmentation was irrelevant to p53 expression. We next investigated how YY1 regulated the CP-31398-mediated p21 up-regulation with siRNA-mediated YY1 down-regulation (Figure 10C). TE-1, TE-10 and TE-11 cells decreased YY1 expression with YY1-siRNA but not with control siRNA. Down-regulation of YY1 increased p21 expression in TE-1 and TE-11 cells but decreased the expression in TE-10 cells when they were treated with CP-31398. TE-10 cells treated with CP-31398 exceptionally increased YY1 expression in contrast with the other cells and showed p21 augmentation like the others (Figure 9A and 9B). These data indicated that YY1 was a negative regulator for p21 expression in CP-31398-treated cells except TE-10 cells of which p21 was positively controlled by YY1. We noticed that knockdown of YY1 did not increase p21 expression in CP-31398-untreated cells and TE-10 cells treated with control siRNA by itself increased YY1 expression but did not influence p21 expression. These data suggested that p21 expression was not totally dependent on YY1 and that regulation of YY1 in TE-10 cells was different from that in the other cells.

Up-regulated p21 mediated CP-31398-induced cell cycle changes

We examined how the up-regulated p21 expression contributed to cell cycle changes induced in CP-31398-treated cells with siRNA-mediated p21 knockdown (Figure 11).

Expression of p21 became completely negative with the siRNA even in CP-31398-treated cells (Figure 11A). Cell cycle progression induced by CP-31398 was examined in cells treated with the siRNA (Figure 11B, Table 3). Increased G2/M fractions observed in TE-1 cells treated with CP-31398 for 48 hrs were not detected in cells treated with p21-siRNA. Likewise, TE-2 cells increased G2/M population with CP31398 treatments but p21-siRNA treated cells decreased the population to the level of untreated cells. TE-2 cells showed increased hyperploidy with CP-31398 treatments and the up-regulation was disappeared with p21-siRNA treatments. Decreased G0/G1 populations induced by CP-31398, probably accompanied by increased G2/M and hyperploidy fractions, was returned to the level of untreated cells. These data collectively indicated that cell cycle changes caused by CP-31398 was mainly due to increased p21 expression.

2.5 Discussion

The present study examined effects of a p53-stailizing CP-31398 on p53 relevant pathways in human squamous esophageal carcinoma cells bearing the wild-type *p53* or mutated *p53* which was not corrected by CP-31398 functions (10). We showed that CP-31398 did not activated the p53 pathway but up-regulated p21 expression of p21 at the transcription level in a p53-independent manner, and demonstrated firstly to our knowledge that the CP-31398-mediated augmentation of p21 expression was regulated by a transcriptional factor YY1. We also showed that the p21 up-regulation was responsible for cell cycle changes induced by CP-31398 in the esophageal carcinoma cells.

Previous studies showed that CP-31398 augmented p53 expression through stabilizing p53 through inhibiting p53 ubiquitination without inhibiting the p53-MDM2 interactions in *p53* wild-type cells (40). The agents also converted a few types of mutated p53 to wild-type p53 though the binding to the p53-DNA binding domain (6, 10). Nevertheless, subsequent studies demonstrated that CP-31398-mediated effects were complex (41) and were dependent on tumors tested and the genetic backgrounds (42). The present study investigated CP-31398-mediated effects in p53-dyfunctional but not p53-deleted tumors on the susceptibility to apoptosis and demonstrated that CP-31398-mediated p53 and the phosphorylation levels and the cytotoxicity were irrelevant to the *p53* genotype, and cleavages of PARP and caspase-3 were not associated with p53 up-regulations. These data therefore indicated that these esophageal carcinoma cells were defective of p53 up-stream pathways as well as p53 down-stream pathway,

and suggested that CP-31398 induced cell death and cell cycle changes were at least partly attributable to non-p53 pathways. Expression profiles of p53 induced by CP-31398 was different from those by CDDP, but the profile changes in p63 and p73 were similar to those by CDDP. The CP-31398-mediated DNA damage responses might thereby be shared to some extent with CDDP in these cells.

We demonstrated in the present study that p21 expression was up-regulated by CP-31398 in contrast to CDDP-induced p21 down-regulation. The up-regulation was irrelevant to activation of the p53 pathway and knockdown of p53 with siRNA confirmed the p53-independent response. We therefore investigated a possible mechanism involved in non-p53-mediated p21 augmentation. Previous studies showed that CP-31398 induced p21 expression in a p53-independent manner (9) but this is the first report to indicate that CP-31398 influenced YY1 expression and regulated p21 expression. YY1 is a transcriptional factor ubiquitously expressed and regulates a number of genes positively or negatively depending on co-factors involved in the regulation (43, 44), and the over-expression was often associated with tumorigenesis and tumor progression including esophageal carcinoma (45). YY1 promoted functions and expression of oncogenes (44), and inhibition of YY1 therefore suppressed cell invasion and metastatic potentials (46). We showed with CP-31398 treated cells that YY1 expression was reversely correlated with p21 expression and furthermore demonstrated that knockdown of YY1 expression augmented the p21 levels. Up-regulation of p21 contributed to cell growth suppression and YYI down-regulation therefore played a role in inhibiting tumorigenic potentials. Previous studies showed

that YY1 inhibited p21 transcription by blocking an access of other factors to the regulatory sequences in p53 wild-type cells (38, 39), but the present study also demonstrated the YY1-mediated p21 regulation in p53 dysfunctional cells. TE-10 cells were exception in the CP-31398- and YYI siRNA-treated studies, which showed that YY1 expression was positively associated with p21 expression and knockdown of YY1 rather decreased p21 expression. Contradictory effects of YY1 on p21 expression found between TE-10 cells and the other cells can be due to differential co-factors engagement in the p21 transcriptions. Nevertheless, these results of TE-10 cells also showed that YY1 regulated p21 expression in CP-31398-treated cells.

We examined other possible factors involved in p53-independent p21 regulation. YY2, a transcription factor belonging to the YY family, is similar to YY1 in the DNA sequences and reciprocally regulated expression of YY1 target genes by competing a binding site at the transcriptional regulatory region (47). YY2 therefore stroked a balance of the target gene expression with YY1. The present data however showed changes of YY2 expression by CP-31398 were unrelated with those of YY1, indicating that YY2 played a minor role in the p21 regulation. A recent study however showed an example of YY2-mediated gene regulation without YY1 involvement, and demonstrated that YY2 increased p53 transcripts through regulation at non-YY1 binding site, and consequently augmented p21 expression (37). YY1 also regulated p53 expression in a different manner from YY2, which included facilitation of p53 ubiquitination by increasing binding between p53 and MDM2 (48-50). The current study did not however showed any correlation between p53 and YY1 or YY2

expression levels in the esophageal carcinoma cells. Interestingly, TE-10 cells exceptionally increased YY1 with CP-31398, and also greatly up-regulated YY2 expression in comparison with other cells showing constant YY2 expression after the CP-31398 treatment. It is however currently unknown how the YY2 increase in TE-10 cells contributed the p21 augmentation under increased YY1 expression.

We also investigated a possible contribution of mTORC1 pathway to p21 expression in a p53-independent manner. Phosphorylation of 4E-BP1, a down-stream molecule of mTORC1, stabilized p21, but the non-phosphorylated form degraded p21 (25). On the contrary, activated mTORC1 inhibited MDM2 functions through p70S6K, and increased p21 levels in a p53-dependent manner (51). The present study examined AMPK, an up-stream pathway of mTORC1, and 4E-BP1 and p70S6K after CP-31398 stimulation. Phosphorylated AMPK induced phosphorylation of 4E-BP1 and p70S6K in cells which had intact AMPK-mTORC1-4E-BP1/p70S6K pathways, but a majority of the esophageal carcinoma cells showed different phosphorylation profiles regarding respective molecules. These data indicated that the majority had distorted signaling in the pathways and the p21 up-regulation was not attributable to phosphorylated 4E-BP1 in these cells.

Esophageal carcinoma cells treated with CP-31398 showed increased G2/M populations to a lesser extent sub-G1 and hyperploidy fractions. We firstly reported to our knowledge that CP-31398 augmented G2/M fractions although increased sub-G1 and G0/G1 populations by CP-31398 were previously reported (9, 52). These cell cycle changes induced by CP-31398 were primarily due to augmented p53 levels but the

present study also showed that the changes were generated without p53 involvement. We also firstly showed that CP-31398 also increased hyperploidy fractions in several cell types, which was caused by aberrant cell division processed and might be precedent for cell death by CP-31398. Cell cycle arrest at G2/M is often associated with increased p27 but the present study showed that increased p27 was irrelevant, but p21 was attributable to the cell cycle changes. Inhibition of cyclin B1-Cdk1 complex and degradation of cyclins A2 and B1 induced by p21 promoted cell cycle arrest at G2 and G2/M phase (53, 54). We did not analyze a mechanism of p21-induced G2/M arrest by CP-31398, but p21 siRNA released the cell cycle arrest and decreased sub-G1 fraction. The data indicated that CP-31398-mediated cell cycle changes were at least due to the up-regulated p21 expression.

In conclusions, we investigated CP-31398-mediated effects on p53 dysfunctional tumors and showed that the agent activated p21 expression at the transcriptional levels. The present study demonstrated that the p21 augmented expression was linked with deceased YY1 without involvement of p53, YY2 or mTORC signaling. We also showed that cell cycle changes induced by CP-31398 was attributable to the YY1-mediated increased p21 levels. The present study firstly demonstrated that a cytotoxic agent, CP-31398, targeted YY1 which was often over-expressed in tumors, and suggested that the CP-31398-mediated effects including the cytotoxicity were attributable to decreased YY1 levels in a p53 dysfunctional tumors.

References

1. Lee AY, Raz DJ, He B, Jablons DM. Update on the molecular biology of malignant mesothelioma. Cancer. 2007;109:1454-61.
2. Katzman D, Sterman DH. Updates in the diagnosis and treatment of malignant pleural mesothelioma. Curr Opin Pulm Med. 2018;24:319-26.
3. Guo G, Chmielecki J, Goparaju C, Heguy A, Dolgalev I, et al. Whole-exome sequencing reveals frequent genetic alterations in BAP1, NF2, CDKN2A, and CUL1 in malignant pleural mesothelioma. Cancer Res. 2015;75:264-9.
4. Bueno R, Stawiski EW, Goldstein LD, Durinck S, De Rienzo A, et al. Comprehensive genomic analysis of malignant pleural mesothelioma identifies recurrent mutations, gene fusions and splicing alterations. Nat Genet. 2016;48:407-16. doi:10.1038/ng.3520.
5. Shen J, Cao B, Wang Y, Ma C, Zeng Z, et al. Hippo component YAP promotes focal adhesion and tumour aggressiveness via transcriptionally activating THBS1/FAK signalling in breast cancer. J Exp Clin Cancer Res. 2018;37:175. doi:10.1186/s13046-018-0850-z.
6. Foster BA, Coffey HA, Morin MJ, Rastinejad F. Pharmacological rescue of mutant p53 conformation and function. Science. 1999;286:2507-10.
7. Tang X, Zhu Y, Han L, Kim AL, Kopelovich L, Bickers DR, Athar M. CP-31398 restores mutant p53 tumor suppressor function and inhibits UVB-induced skin carcinogenesis in mice. J Clin Invest. 2007;117:3753–64.
8. Rippin TM, Bykov VJ, Freund SM, Selivanova G, Wiman KG, Fersht AR.

Characterization of the p53-rescue drug CP-31398 in vitro and in living cells. Oncogene. 2002;21:2119-29.

9. Takimoto R, Wang W, Dicker DT, Rastinejad F, Lyssikatos J, el-Deiry WS. The mutant p53-conformation modifying drug, CP-31398, can induce apoptosis of human cancer cells and can stabilize wild-type p53 protein. Cancer Biol Ther. 2002;1:47-55.
10. Demma MJ, Wong S, Maxwell E, Dasmahapatra B. CP-31398 restores DNA-binding activity to mutant p53 in vitro but does not affect p53 homologs p63 and p73. J Biol Chem. 2004;279:45887–96.
11. Van Maerken T, Ferdinande L, Taildeman J, Lambertz I, Yigit N, et al. Antitumor activity of the selective MDM2 antagonist nutlin-3 against chemoresistant neuroblastoma with wild-type p53. J Natl Cancer Inst. 2009;101:1562-74.
12. Hopkins-Donaldson S, Belyanskaya LL, Simões-Wüst AP, Sigrist B, Kurtz S, Zangemeister-Wittke U, Stahel R. p53-induced apoptosis occurs in the absence of p14(ARF) in malignant pleural mesothelioma. Neoplasia. 2006;8:551-9.
13. Shapiro IM, Kolev VN, Vidal CM, Kadariya Y, Ring JE, et al. Merlin deficiency predicts FAK inhibitor sensitivity: a synthetic lethal relationship. Sci Transl Med. 2014;6:237ra68. doi:10.1126/scitranslmed.3008639.
14. Soria JC, Gan HK, Blagden SP, Plummer R, Arkenau HT, et al. A phase I, pharmacokinetic and pharmacodynamic study of GSK2256098, a focal adhesion kinase inhibitor, in patients with advanced solid tumors. Ann Oncol. 2016;27:2268-74.

15. Lim ST, Chen XL, Lim Y, Hanson DA, Vo TT, Howerton K, Larocque N, Fisher SJ, Schlaepfer DD, Ilic D. Nuclear FAK promotes cell proliferation and survival through FERM-enhanced p53 degradation. Mol Cell. 2008;29:9-22.

16. Ammoun S, Schmid MC, Zhou L, Hilton DA, Barczyk M, Hanemann CO. The p53/mouse double minute 2 homolog complex deregulation in merlin-deficient tumours. Mol Oncol. 2015;9:236-48.

17. Golubovskaya VM, Finch R, Cance WG. Direct interaction of the N-terminal domain of focal adhesion kinase with the N-terminal transactivation domain of p53. J Biol Chem. 2005;280:25008-21.

18. Golubovskaya VM, Finch R, Kweh F, Massoll NA, Campbell-Thompson M, Wallace MR, Cance WG. p53 regulates FAK expression in human tumor cells. Mol Carcinog. 2008;47:373-82.

19. Nakataki E, Yano S, Matsumori Y, Goto H, Kakiuchi S, et al. Novel orthotopic implantation model of human malignant pleural mesothelioma (EHMES-10 cells) highly expressing vascular endothelial growth factor and its receptor. Cancer Sci. 2006;97:183-91.

20. Di Marzo D, Forte IM, Indovina P, Di Gennaro E, Rizzo V, et al. Pharmacological targeting of p53 through RITA is an effective antitumoral strategy for malignant pleural mesothelioma. Cell Cycle. 2014;13:652-65.

21. Fiorini C, Menegazzi M, Padroni C, Dando I, Dalla Pozza E, Gregorelli A, Costanzo C, Palmieri M, Donadelli M. Autophagy induced by p53-reactivating molecules protects pancreatic cancer cells from apoptosis. Apoptosis. 2013;18:337–46.

22. Wang W, Rastinejad F, El-Deiry WS. Restoring p53-dependent tumor suppression. Cancer Biol Ther. 2003;2:S55-63.

23. Bassett EA, Wang W, Rastinejad F, El-Deiry WS. Structural and functional basis for therapeutic modulation of p53 signaling. Clin Cancer Res. 2008;14:6376-86.

24. Luu Y, Bush J, Cheung KJ Jr, Li G. The p53 stabilizing compound CP-31398 induces apoptosis by activating the intrinsic Bax/mitochondrial/caspase-9 pathway. Exp Cell Res. 2002;276:214-22.

25. Llanos S, Garc á-Pedrero JM, Morgado-Palacin L, Rodrigo JP, Serrano M. Stabilization of p21 by mTORC1/4E-BP1 predicts clinical outcome of head and neck cancers. Nat Commun. 2016;7:10438. doi:10.1038/ncomms10438.

26. Matsuda T, Kato T, Kiyotani K, Tarhan YE, Saloura V, Chung S, Ueda K, Nakamura Y, Park JH. p53-independent p21 induction by MELK inhibition. Oncotarget. 2017;8:57938-47.

27. Gartel AL, Tyner AL. The role of the cyclin-dependent kinase inhibitor p21 in apoptosis. Mol Cancer Ther. 2002;1:639-49.

28. Weaver JMJ, Ross-Innes CS, Shannon N, Lynch AG, Forshew T, et al. Ordering of mutations in preinvasive disease stages of esophageal carcinogenesis. Nat Genet. 2014;46:837-43.

29. Sawada G, Niida A, Uchi R, Hirata H, Shimamura T, et al. Genomic landscape of esophageal squamous cell carcinoma in a Japanese population. Gastroenterology. 2016;150:1171–82.

30. Gao YB, Chen ZL, Li JG, Hu XD, Shi XJ, et al. Genetic landscape of esophageal

squamous cell carcinoma. Nat Genet. 2014;46:1097-102.

31. Hong B, van den Heuvel AP, Prabhu VV, Zhang S, El-Deiry WS. Targeting tumor suppressor p53 for cancer therapy: strategies, challenges and opportunities. Current Drug Targets. 2014;15:80-89.
32. Zandi R, Selivanova G, Christensen CL, Gerds TA, Willumsen BM, Poulsen HS. PRIMA-1Met/APR-246 induces apoptosis and tumor growth delay in small cell lung cancer expressing mutant p53. Clin Cancer Res. 2011;17:2830-41.
33. He T, Guo J, Song H, Zhu H, Di X, et al. Nutlin-3, an antagonist of MDM2, enhances the radiosensitivity of esophageal squamous cancer with wild-type p53. Pathol Oncol Res. 2018;24:75-81.
34. Ma G, Kawamura K, Li Q, Suzuki N, Liang M, Namba M, Shimada H, Tagawa M. Cytotoxicity of adenoviruses expressing the wild-type p53 gene to esophageal carcinoma cells is linked with the CAR expression level and indirectly with the endogenous p53 status. Cancer Gene Ther. 2009;16:832-40.
35. Shimada H, Nabeya Y, Tagawa M, Okazumi S, Matsubara H, et al. Preoperative serum midkine concentration is a prognostic marker for esophageal squamous cell carcinoma. Cancer Sci. 2003;94:628-32.
36. Drakos E, Thomaides A, Medeiros LJ, Li J, Leventaki V, Konopleva M, Andreeff M, Rassidakis GZ. Inhibition of p53-murine double minute 2 interaction by nutlin-3A stabilizes p53 and induces cell cycle arrest and apoptosis in Hodgkin lymphoma. Clin Cancer Res. 2007;13:3380-7.
37. Kasim V, Xie YD, Wang HM, Huang C, Yan XS, Nian WQ, Zheng XD, Miyagishi

M, Wu SR. Transcription factor Yin Yang 2 is a novel regulator of the p53/p21 axis. Oncotarget. 2017;8:54694-707.

38. Ishii H, Hulett MD, Li JM, Santiago FS, Parish CR, Khachigian LM. Yin Yang-1 inhibits tumor cell growth and inhibits p21WAF1 / Cip1 complex formation with Cdk4 and Cyclin D1. Int J Oncol. 2012;40:1575–80.
39. Santiago FS, Ishii H, Shafi S, Khurana R, Kanellakis P, et al. Yin Yang-1 inhibits vascular smooth muscle cell growth and intimal thickening by repressing p21WAF1 / Cip1 transcription and p21WAF1 / Cip1-Cdk4-Cyclin D1 assembly. Circ Res. 2007;101:146–55.
40. Wang W, Takimoto R, Rastinejad F, El-Deiry WS. Stabilization of p53 by CP-31398 inhibits ubiquitination without altering phosphorylation at serine 15 or 20 or MDM2 binding. Mol Cell Biol. 2003;23:2171-81.
41. Tanner S, Barberis A. CP-31398, a putative p53-stabilizing molecule tested in mammalian cells and in yeast for its effects on p53 transcriptional activity. J Negat Results Biomed. 2004;3:5.
42. Ho CK, Li G. Mutant p53 melanoma cell lines respond differently to CP-31398-induced apoptosis. Brit J Dermatol. 2005;153:900–10.
43. Deng Z, Cao P, Wan MM, Sui G. Yin Yang 1: a multifaceted protein beyond a transcription factor. Transcription. 2010;1:81-4.
44. Zhang Q, Stovall DB, Inoue K, Sui G. The Oncogenic Role of Yin Yang 1. Crit Rev Oncog. 2011;16:163–97.
45. Luo J, Jiang X, Cao L, Dai K, Zhang S, Ge X, Zhou X, Lu X. Expression of YY1

correlates with progression and metastasis in esophageal squamous cell carcinomas. Onco Targets Ther. 2014;7:1753-9.

46. de Nigris F, Rossiello R, Schiano C, Arra C, Williams-Ignarro S, et al. Deletion of Yin Yang 1 protein in osteosarcoma cells on cell invasion and CXCR4/angiogenesis and metastasis. Cancer Res. 2008;68:1797-808.
47. Nguyen N, Zhang X, Olashaw N, Seto E. Molecular cloning and functional characterization of the transcription factor YY2. J Biol Chem. 2004;279:25927-34.
48. Sui G, Affar el B, Shi Y, Brignone C, Wall NR, et al. Yin Yang 1 is a negative regulator of p53. Cell. 2004;117:859–72.
49. Gronroos E, Terentiev AA, Punga T, Ericsson J. YY1 inhibits the activation of the p53 tumor suppressor in response to genotoxic stress. Proc Natl Acad Sci U S A. 2004;101:12165–70.
50. Castellano G, Torrisi E, Ligresti G, Malaponte G, Militello L, Russo AE, McCubrey JA, Canevari S, Libra M. The involvement of the transcription factor Yin Yang 1 in cancer development and progression. Cell Cycle. 2009;8:1367-72.
51. Lai KP, Leong WF, Chau JF, Jia D, Zeng L, et al. S6K1 is a multifaceted regulator of Mdm2 that connects nutrient status and DNA damage response. EMBO J. 2010;29:2994-3006.
52. Wischhusen J, Naumann U, Ohgaki H, Rastinejad F, Weller M. CP-31398, a novel p53-stabilizing agent, induces p53-dependent and p53-independent glioma cell death. Oncogene. 2003;22:8233–45.
53. Charrier-Savournin FB, Château MT, Gire V, Sedivy J, Piette J, Dulic V. p21-

Mediated nuclear retention of cyclin B1-Cdk1 in response to genotoxic stress. Mol Biol Cell. 2004;15:3965-76.

54. Lee J, Kim JA, Barbier V, Fotedar A, Fotedar R. DNA damage triggers p21WAF1-dependent Emi1 down-regulation that maintains G2 arrest. Mol Biol Cell. 2009;20:1891-902.

Table 1 Cell cycle distribution of mesothelioma cells treated with CP-31398, nutlin-3a or the combination.

Cells	Agent	Cell cycle distribution (%) (Average ± SE)			
		Sub-G1	G1	S	G2/M
MSTO-211H	(-)	0.58 ± 0.04	91.54 ± 0.16	2.34 ± 0.16	5.54 ± 0.03
	CP-31398	4.44 ± 0.97	67.76 ± 0.96	8.53 ± 0.52	19.26 ± 0.92
	Nutlin-3a	4.08 ± 0.49	85.75 ± 0.50	1.02 ± 0.15	9.15 ± 0.81
	CP-31398 + Nutlin-3a	12.28 ± 0.29	46.99 ± 0.26	23.39 ± 0.08	17.34 ± 0.49
NCI-H28	(-)	2.79 ± 0.08	79.12 ± 0.37	8.56 ± 0.09	9.53 ± 0.25
	CP-31398	1.96 ± 0.38	73.09 ± 2.58	9.24 ± 0.12	15.71 ± 1.56
	Nutlin-3a	7.25 ± 2.15	85.69 ± 1.80	3.84 ± 0.27	3.22 ± 0.54
	CP-31398 + Nutlin-3a	3.54 ± 0.46	70.19 ± 1.29	9.49 ± 1.13	16.78 ± 0.62

Cells were treated with CP-31398 (15 μM), nutlin-3a (10 μM) or the combination for 48 hrs and the cell cycle was analyzed with FACSCalibur.

Table 2 Cell cycle progression of esophageal carcinoma cells treated with CP-31398

Cells	Time (hrs)	CP-31398 (μM)	Cell cycle distribution (%) (Average ± SE)				
			Sub-G1	G1	S	G2/M	Hyperploidy
TE-1	24	(-)	1.43 ± 0.03	43.57 ± 1.13	22.02 ± 0.53	27.80 ± 0.35	5.19 ± 0.03
		3	2.20 ± 0.19	62.86 ± 0.69	15.50 ± 0.67	16.98 ± 2.16	2.46 ± 0.01
		10	2.83 ± 0.12	38.22 ± 0.38	11.57 ± 0.43	41.60 ± 0.38	5.77 ± 0.05
	48	(-)	1.30 ± 0.03	57.30 ± 0.29	10.45 ± 0.22	25.57 ± 0.10	5.38 ± 0.10
		3	1.05 ± 0.03	54.08 ± 0.69	14.00 ± 0.30	25.14 ± 0.17	5.74 ± 0.07
		10	3.87 ± 0.17	37.94 ± 0.07	8.07 ± 0.10	43.82 ± 0.30	6.30 ± 0.03
TE-2	24	(-)	4.13 ± 0.05	31.95 ± 0.44	22.68 ± 0.20	35.23 ± 0.22	6.01 ± 0.02
		3	3.31 ± 0.13	20.29 ± 0.20	26.84 ± 0.20	37.79 ± 0.26	11.77 ± 0.05
		10	3.31 ± 0.14	14.93 ± 0.21	20.12 ± 0.17	47.48 ± 0.35	14.16 ± 0.07
	48	(-)	3.32 ± 0.11	32.32 ± 0.41	23.80 ± 0.09	34.64 ± 0.33	5.92 ± 0.12
		3	4.54 ± 0.13	26.01 ± 0.20	22.68 ± 0.19	35.55 ± 0.23	11.22 ± 0.04
		10	6.97 ± 0.19	11.39 ± 0.61	15.71 ± 0.24	47.30 ± 0.15	18.64 ± 0.15
TE-10	24	(-)	1.09 ± 0.02	44.26 ± 0.50	23.00 ± 0.45	29.86 ± 0.42	1.79 ± 0.02
		3	1.67 ± 0.14	45.46 ± 0.40	25.54 ± 0.33	26.23 ± 0.23	1.00 ± 0.06
		10	3.81 ± 0.20	34.58 ± 0.46	35.04 ± 0.13	24.67 ± 0.55	1.90 ± 0.05
	48	(-)	1.35 ± 0.02	55.77 ± 0.20	20.26 ± 0.24	21.68 ± 0.16	0.94 ± 0.02
		3	1.82 ± 0.16	52.90 ± 0.40	22.03 ± 0.09	21.92 ± 0.20	1.33 ± 0.01

		10	4.68 ±0.13	27.84 ±0.23	23.86 ±0.61	39.54 ±0.33	4.08 ±0.15
TE-11	24	(-)	42.47 ±0.19	33.65 ±0.20	14.77 ±0.28	8.89 ±0.37	0.23 ±0.02
		3	48.38 ±0.41	28.21 ±0.30	15.89 ±0.32	7.33 ±0.48	0.19 ±0.03
		10	39.56 ±0.11	29.15 ±0.25	18.17 ±0.12	12.19 ±0.09	0.93 ±0.01
	48	(-)	48.54 ±0.44	33.17 ±0.47	10.86 ±0.28	7.10 ±0.29	0.32 ±0.01
		3	48.99 ±0.27	29.93 ±0.30	12.42 ±0.10	8.05 ±0.06	0.61 ±0.01
		10	39.56 ±0.14	28.76 ±0.46	16.68 ±0.13	13.37 ±0.22	1.63 ±0.04
YES-2	24	(-)	1.93 ±0.06	45.75 ±0.27	25.96 ±0.20	25.96 ±0.25	0.40 ±0.01
		3	1.95 ±0.20	47.74 ±0.73	23.13 ±0.52	26.56 ±0.84	0.62 ±0.03
		10	2.88 ±0.10	36.64 ±0.44	32.74 ±0.29	23.61 ±0.38	4.13 ±0.05
	48	(-)	2.87 ±0.01	52.52 ±0.32	25.79 ±0.24	18.20 ±0.15	0.62 ±0.02
		3	2.36 ±0.37	46.14 ±0.73	29.03 ±0.12	21.38 ±1.08	1.09 ±0.03
		10	6.39 ±0.23	26.08 ±0.82	35.64 ±0.24	26.37 ±0.27	5.52 ±0.04
YES-4	24	(-)	16.40 ±0.79	48.61 ±0.36	22.06 ±0.20	12.43 ±0.80	0.50 ±0.01
		3	14.95 ±0.29	45.48 ±0.24	23.33 ±0.51	15.86 ±0.04	0.38 ±0.05
		10	14.64 ±0.19	39.63 ±0.09	22.11 ±0.17	22.12 ±0.22	1.49 ±0.05
	48	(-)	15.29 ±0.12	49.45 ±0.42	21.84 ±0.26	12.39 ±0.38	1.03 ±0.04
		3	16.54 ±0.05	48.06 ±0.24	21.08 ±0.17	13.20 ±0.03	1.13 ±0.01
		10	15.41 ±0.10	35.16 ±0.46	19.48 ±0.01	27.65 ±0.34	2.29 ±0.04
YES-5	24	(-)	2.25 ±0.07	44.09 ±0.57	25.03 ±0.47	23.45 ±0.33	5.19 ±0.03
		3	3.49 ±0.07	49.18 ±0.06	21.21 ±0.14	19.57 ±0.28	6.55 ±0.12

		10	9.83 ±0.27	31.51 ±0.83	22.01 ±0.73	32.24 ±0.42	4.41 ±0.03
	48	(-)	3.39 ±0.14	47.04 ±0.37	24.38 ±0.17	20.42 ±0.03	4.77 ±0.02
		3	3.30 ±0.09	48.79 ±0.06	23.09 ±0.12	20.57 ±0.08	4.24 ±0.10
		10	5.21 ±0.04	47.38 ±0.11	12.71 ±0.11	26.80 ±0.29	7.90 ±0.05
YES-6	24	(-)	2.25 ±0.03	48.63 ±0.31	21.38 ±0.13	27.10 ±0.14	0.64 ±0.02
		3	1.69 ±0.13	48.32 ±0.18	20.02 ±0.20	29.17 ±0.49	0.81 ±0.04
		10	1.90 ±0.10	48.07 ±0.21	18.11 ±0.29	30.70 ±0.37	1.22 ±0.03
	48	(-)	2.69 ±0.09	64.27 ±0.28	11.16 ±0.04	21.20 ±0.22	0.68 ±0.03
		3	2.75 ±0.06	61.41 ±0.18	11.11 ±0.19	23.42 ±0.02	1.32 ±0.10
		10	9.29 ±0.15	49.34 ±0.52	12.47 ±0.04	27.20 ±0.37	1.69 ±0.05
T.Tn	24	(-)	2.48 ±0.07	57.91 ±0.09	20.06 ±0.13	17.83±0.09	1.73 ±0.02
		3	3.78 ±0.08	62.78 ±0.15	19.22 ±0.42	12.70 ±0.31	1.52 ±0.04
		10	12.37 ±0.23	27.16 ±0.04	23.59 ±0.39	25.33 ±0.28	11.55 ±0.03
	48	(-)	2.61 ±0.04	62.33 ±0.33	19.24 ±0.30	14.19 ±0.11	1.64 ±0.03
		3	4.12 ±0.06	61.50 ±0.15	18.69 ±0.13	13.54 ±0.04	2.16 ±0.10
		10	22.34 ±0.16	17.82 ±0.32	27.85 ±0.21	15.77 ±0.52	16.23 ±0.05

Cells treated with CP-31398 was analyzed for the cell cycle progression with a flow cytometry.

Table 3 Cell cycle progression of p21 down-regulated esophageal carcinoma cells which were treated with CP-31398

Cells	Time (hrs)	Conditions	Cell cycle distribution (%) (Average ± SE)				
			Sub-G1	G1	S	G2/M	Hyperploidy
TE-1	24	(-)	5.21 ± 0.14	44.96 ± 0.68	14.41 ± 0.25	28.11 ± 0.29	7.32 ± 0.01
		Control siRNA	5.45 ± 0.12	43.70 ± 0.37	14.40 ± 0.11	29.03 ± 0.47	7.41 ± 0.03
		Control siRNA + CP-31398	6.14 ± 0.04	40.95 ± 0.37	12..88 ± 0.10	32.35 ± 0.30	7.69 ± 0.14
		p21-siRNA	5.00 ± 0.10	44.01 ± 0.31	14.56 ± 0.05	29.01 ± 0.30	7.42 ± 0.30
		p21-siRNA + CP-31398	4.17 ± 0.03	44.98 ± 0.14	14.49 ± 0.11	28.82 ± 0.07	7.55 ± 0.14
	48	(-)	2.65 ± 0.23	42.29 ± 0.82	16.96 ± 0.58	27.10 ± 0.06	11.00 ± 0.01
		Control siRNA	2.81 ± 0.14	40.93 ± 0.41	17.77 ± 0.17	26.57 ± 0.24	11.92 ± 0.11
		Control siRNA + CP-31398	4.06 ± 0.02	31.51 ± 0.26	19.40 ± 0.51	31.71 ± 0.67	13.34 ± 0.01
		p21-siRNA	1.92 ± 0.05	39.90 ± 0.35	17.99 ± 0.36	27.18 ± 0.11	13.01 ± 0.20
		p21-siRNA + CP-31398	2.66 ± 0.08	41.11 ± 0.30	17.54 ± 0.33	25.70 ± 0.35	12.99 ± 0.03
TE-2	24	(-)	2.59 ± 0.04	29.66 ± 0.17	29.81 ± 0.14	34.11 ± 0.16	3.83 ± 0.02
		Control siRNA	2.20 ± 0.08	33.53 ± 0.35	30.00 ± 0.04	31.37 ± 0.41	2.90 ± 0.07

	Control siRNA + CP-31398	4.35 ± 0.03	30.88 ± 0.69	15.88 ± 0.30	38.73 ± 0.17	10.16 ± 0.07
	p21-siRNA	4.26 ± 0.28	32.26 ± 0.44	27.07 ± 0.62	30.69 ± 0.38	5.72 ± 0.05
	p21-siRNA + CP-31398	5.01 ± 0.26	33.10 ± 1.13	25.94 ± 0.23	30.38 ± 0.40	5.57 ± 0.07
48	(-)	2.72 ± 0.04	32.21 ± 0.21	39.47 ± 0.06	20.33 ± 0.39	5.27 ± 0.12
	Control siRNA	3.67 ± 0.34	38.03 ± 2.58	34.26 ± 0.37	20.36 ± 1.57	3.68 ± 0.07
	Control siRNA + CP-31398	3.00 ± 0.42	13.08 ± 1.26	36.56 ± 1.42	39.16 ± 1.65	7.48 ± 0.07
	p21-siRNA	4.48 ± 0.07	32.04 ± 1.09	29.38 ± 0.27	25.42 ± 0.64	8.68 ± 0.04
	p21-siRNA + CP-31398	4.61 ± 0.03	33.36 ± 0.35	29.68 ± 0.06	23.26 ± 0.04	9.09 ± 0.15

Cells transfected with p21-siRNA or control siRNA were treated with CP-31398. The cell cycle profiles was analyzed with a flow cytometry.

Figure legends

Figure 1 Growth inhibitory activity and molecular expression induced by CP-31398 in mesothelioma. (a) Cells were treated with various concentrations of CP-31398 for 4 days and the cell viabilities were measured with a colorimetric WST agent. Relative viability was calculated based on untreated cells. IC_{50} values calculated with CalcuSyn software are shown. Averages and SE bars are shown (n=3). (b) Live cell numbers after treated with CP-31398 were counted with a trypan blue dye exclusion assay. Averages and SE bars are shown (n=3). (c) Cells were treated with CP-31398 for 24 hrs and the expression of respective molecules as indicated was analyzed with Western blot analysis. An upper and a lower arrow indicate authentic and truncated p53, respectively. Actin was used as a loading control.

Figure 2. Growth inhibitory activity and molecular expression induced by nutlin-3a in mesothelioma. (a) Cells were treated with various concentrations of nutlin-3a for 4 days and the cell viabilities were measured with a colorimetric WST agent. Relative viability was calculated based on untreated cells. IC_{50} values calculated with CalcuSyn software are shown. Averages and SE bars are shown (n=3). (b) Cells were treated with nutlin-3a for 24 hrs and the expression of respective molecules as indicated was analyzed with Western blot analysis. Actin was used as a loading control.

Figure 3. Growth inhibition caused by a combinatory use of CP-31398 and nultin-3a. (a) Cells were treated with various concentrations of CP-31398 and nutlin-3a with an

indicated concentration, and the cell viabilities were measured with a colorimetric WST agent. Relative viability was calculated based on untreated cells. Averages and SE bars are shown (n=3). CI values in the combination were calculated with CalcuSyn software at various Fa points. (b) Live cell numbers after treated with CP-31398, nutlin-3a or the combination were counted with a trypan blue dye exclusion assay. Averages and SE bars are shown (n=3). Asterisks showed $P<0.01$. (c) Representative profiles of cell cycle distributions after treated with CP-31398 (15 μM), nutrin-3a (10 μM) or the combination for 48 hrs.

Figure 4. Molecular expression in cells treated with combination of CP-31398 and nutlin-3a. Cells were treated with the agent at the indicated concentration for 24 hrs and were subjected to Western blot analysis as indicated. Actin was used as a loading control.

Figure 5. Growth inhibition and molecular expression caused by a combinatory use of CP-31398 and defactinib. (a) Cells were treated with various concentrations of CP-31398 and defactinib with the indicated concentration, and the cell viabilities were measured with a colorimetric WST agent. Relative viability was calculated based on untreated cells. Averages and SE bars are shown (n=3). CI values in the combination were calculated with CalcuSyn software at various Fa points. (b) Cells were treated with the agent at the indicated concentration for 24 hrs and were subjected to Western blot analysis as indicated. Actin was used as a loading control.

Figure 6 Human esophageal carcinoma cells were defective of p53 activation. (A, C) Esophageal carcinoma with the wild-type *p53* (A) and mutated *p53* genotype (C) were treated with CDDP (20 μM) for 24 or 48 hrs, and expression levels of p53 and the relevant molecules were examined with Western blot analysis. Actin was used as a loading control. (B) Expression of *p53* mRNA in CDDP-treated cells. Cells which were untreated or treated with 20 μM of CDDP for 24 hrs were examined for expression of p53 and GAPDH transcripts as a loading control with RT-PCR. (D) Cells were treated with nutlin-3a at various concentrations and the viabilities were measured with the WST assay. IC_{50} values were calculated with CalcuSyn software. Averages and SE bars are shown (n=3). (E) Growth inhibitory effects of nutlin-3a on mesothelioma cells with different *p53* genotype. Cells were treated with nutlin-3a at various concentrations and the cell viabilities were measured with the WST assay. IC_{50} values were calculated with CalcuSyn software. Averages and SE bars are shown (n=3).

Figure 7. CP-31398-mediated effects on esophageal carcinoma. (A, B) Esophageal carcinoma (A) and (B) mesothelioma cells were treated with CP-31398 as indicated and the cell viabilities were measured with the WST assay. IC_{50} values were calculated with CalcuSyn software. Averages and SE bars are shown (n=3). (C) Cells were treated with CP-31398 as indicated and live cell numbers were counted with a trypan blue dye exclusion assay. Averages and SE bars are shown (n=3). (D) Representative cell cycle profiles of esophageal carcinoma cells which were treated with CP-31398 for 48 hrs were analyzed with a flow cytometry. Percentages of each fraction was shown in Table

1. (E) Percentages of G2/M phase populations in esophageal carcinoma treated with CP-31398 as indicated for 48 hrs. SE bars are also shown (n=3). *P<0.05. ns: not significant. The percentages are also shown in Table 2.

Figure 8 Expression of the p53 family and the related molecules in CP-31398-treated cells. Esophageal carcinoma cells were treated with CP-31398 (10 μM) for 48 hrs and subjected to Western blot analysis as indicated. Actin was used as a loading control.

Figure 9 CP-31398-mediated augmentation of p21 and suppression of YY1 expression. Esophageal carcinoma cells treated with CP-31398 (A) at different concentrations as indicated for 48 hrs or (B) at 10μM for different times as indicated, were subjected to Western blot analysis. Actin was used as a loading control.

Figure 10 CP-31398-mediated up-regulation of p21 was independent of p53 but associated with YY1 expression. (A) Esophageal carcinoma cells treated with CP-31398 as indicated for 48 hrs and amounts of *p21* transcripts was analyzed with RT-PCR. GAPDH is shown as a control. (B) Cells transfected with either (B) p53-siRNA or (C) YY1-siRNA were treated with CP-31398 at 10 μM for 48hrs and subjected to Western blot analysis. Cells transfected with control siRNA were also used as a control. Actin was used as a loading control.

Figure 11 CP-31398-mediated cell cycle changes were attributable to augmented p21

expression. (A) Cells transfected with p21-siRNA or control siRNA were treated with CP-31398 at 10 μM for 48 hrs and subjected to Western blot analysis. Actin was used as a loading control. (B) Representative cell cycle profiles of cells treated with siRNA and/or CP-31398 at 10 μM for 48 hrs. The profiles were examined with a flow cytometry. A percentage of each fraction was shown in Table 3.

Figure 1

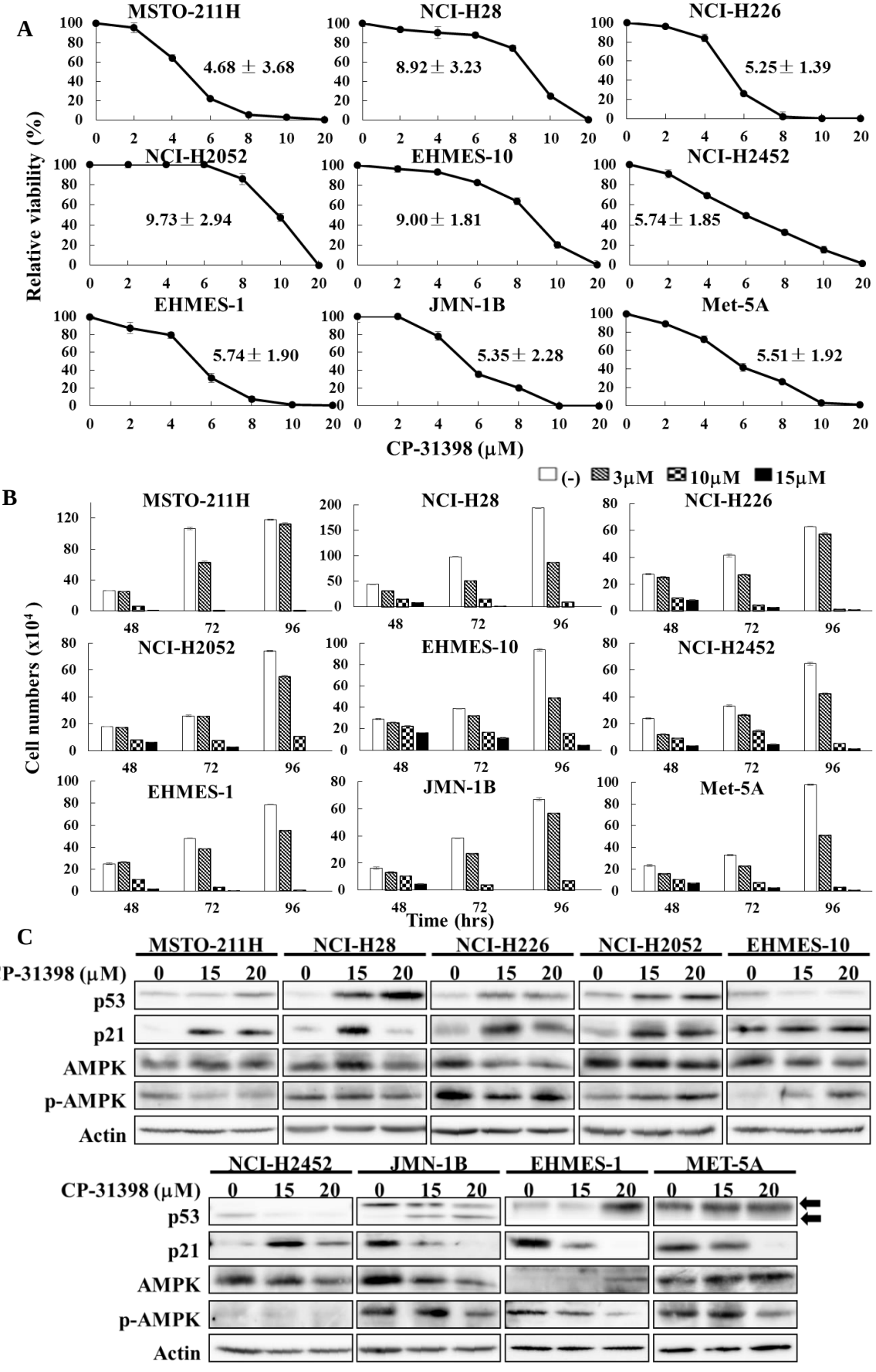
A
MSTO-211H
4.68 ± 3.68
NCI-H28
8.92± 3.23
NCI-H226
5.25± 1.39
NCI-H2052
9.73± 2.94
EHMES-10
9.00± 1.81
NCI-H2452
5.74± 1.85
EHMES-1
5.74± 1.90
JMN-1B
5.35± 2.28
Met-5A
5.51± 1.92
Relative viability (%)
CP-31398 (μM)
B
(-) 3μM 10μM 15μM
MSTO-211H
NCI-H28
NCI-H226
NCI-H2052
EHMES-10
NCI-H2452
EHMES-1
JMN-1B
Met-5A
Cell numbers (x10⁴)
Time (hrs)
C
MSTO-211H
NCI-H28
NCI-H226
NCI-H2052
EHMES-10
CP-31398 (μM) 0 15 20
p53
p21
AMPK
p-AMPK
Actin
NCI-H2452
JMN-1B
EHMES-1
MET-5A
CP-31398 (μM) 0 15 20
p53
p21
AMPK
p-AMPK
Actin

Figure 2

A

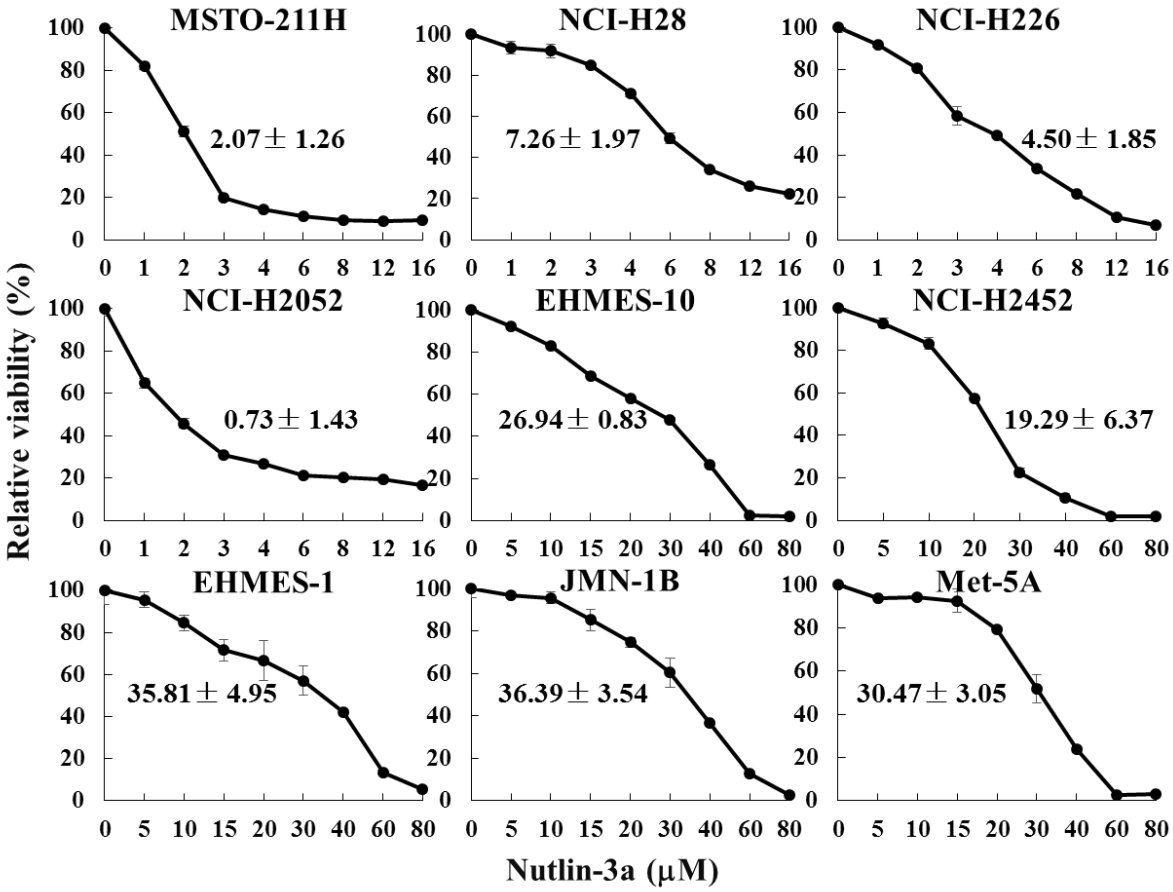
MSTO-211H
2.07± 1.26
NCI-H28
7.26± 1.97
NCI-H226
4.50± 1.85
NCI-H2052
0.73± 1.43
EHMES-10
26.94± 0.83
NCI-H2452
19.29± 6.37
EHMES-1
35.81± 4.95
JMN-1B
36.39± 3.54
Met-5A
30.47± 3.05
Relative viability (%)
Nutlin-3a (μM)

B

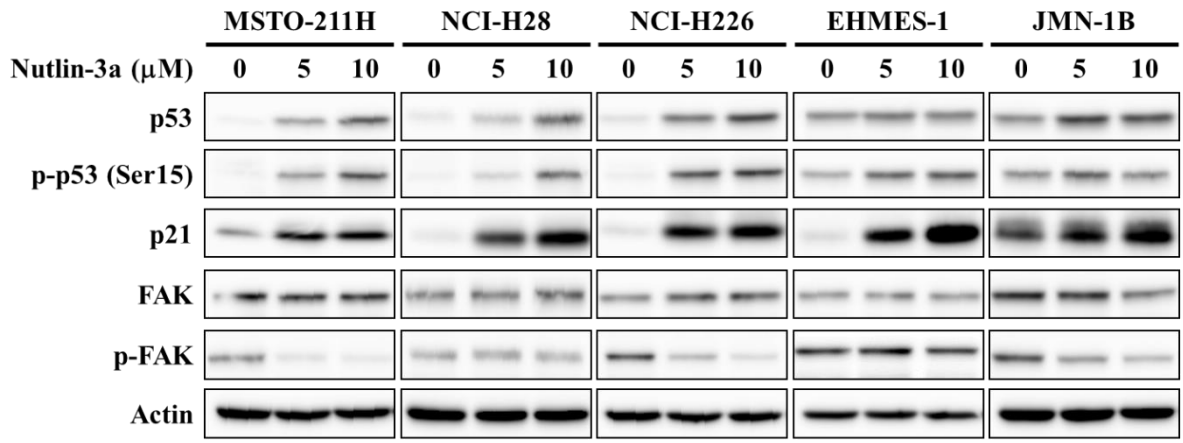
MSTO-211H
NCI-H28
NCI-H226
EHMES-1
JMN-1B
Nutlin-3a (μM)
0 5 10
p53
p-p53 (Ser15)
p21
FAK
p-FAK
Actin

Figure 3

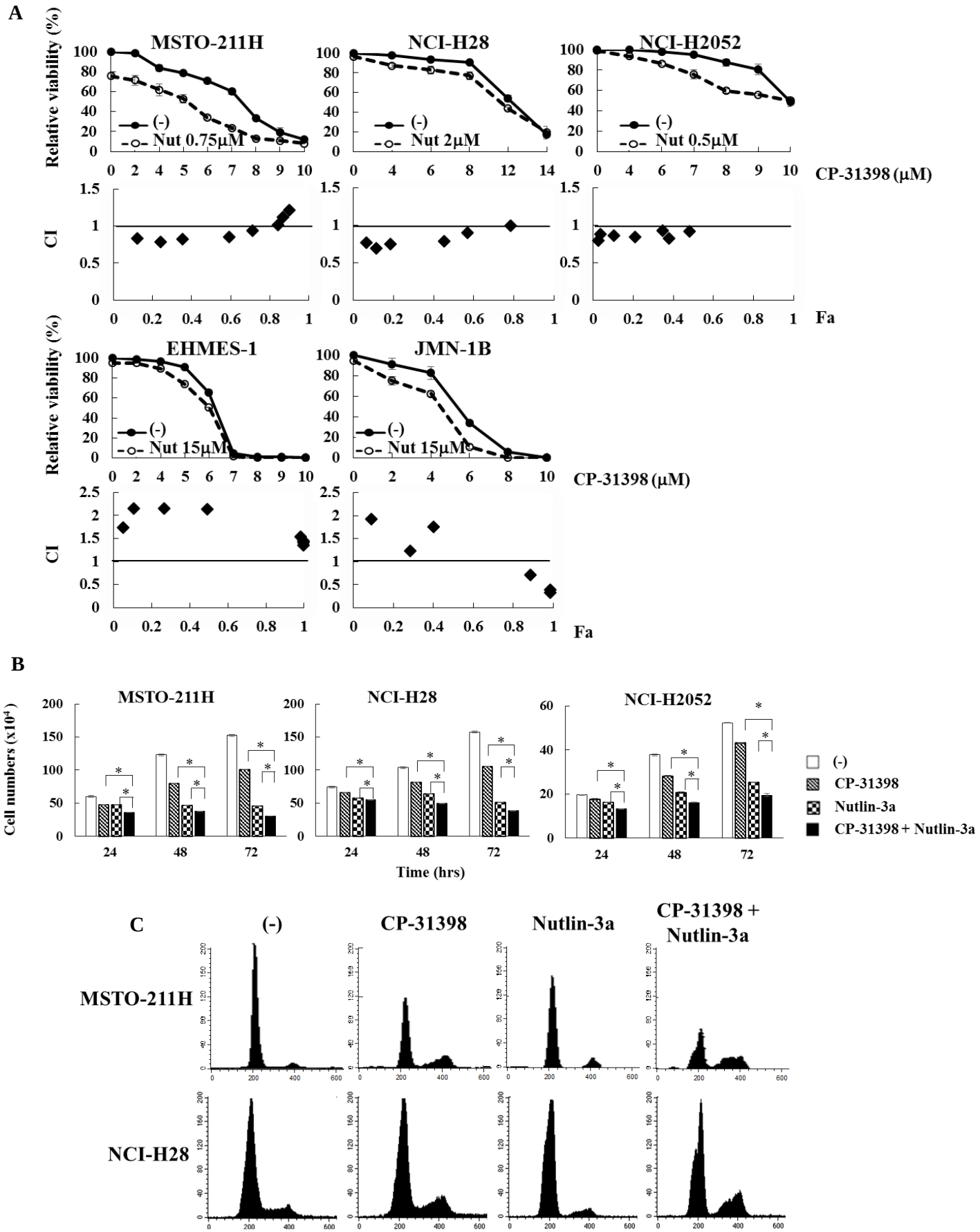
A
MSTO-211H
NCI-H28
NCI-H2052
Relative viability (%)
(-)
Nut 0.75μM
Nut 2μM
Nut 0.5μM
CP-31398 (μM)
CI
Fa
EHMES-1
JMN-1B
Nut 15μM
B
Cell numbers (x10⁴)
Time (hrs)
(-)
CP-31398
Nutlin-3a
CP-31398 + Nutlin-3a
C
(-)
CP-31398
Nutlin-3a
CP-31398 + Nutlin-3a
MSTO-211H
NCI-H28

Figure 4

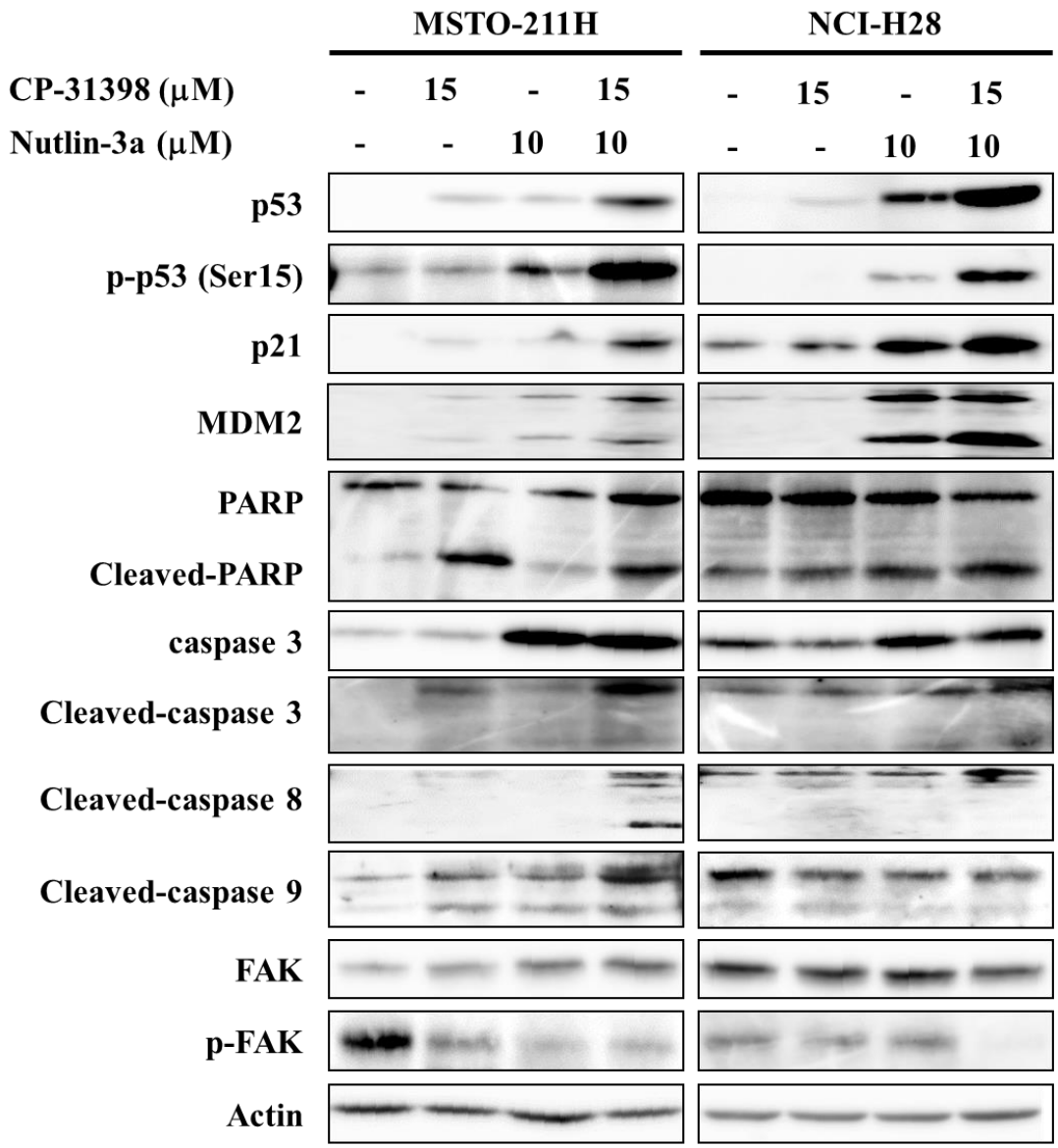
MSTO-211H
NCI-H28
CP-31398 (μM)
- 15 - 15 - 15 - 15
Nutlin-3a (μM)
- - 10 10 - - 10 10
p53
p-p53 (Ser15)
p21
MDM2
PARP
Cleaved-PARP
caspase 3
Cleaved-caspase 3
Cleaved-caspase 8
Cleaved-caspase 9
FAK
p-FAK
Actin

Figure 5

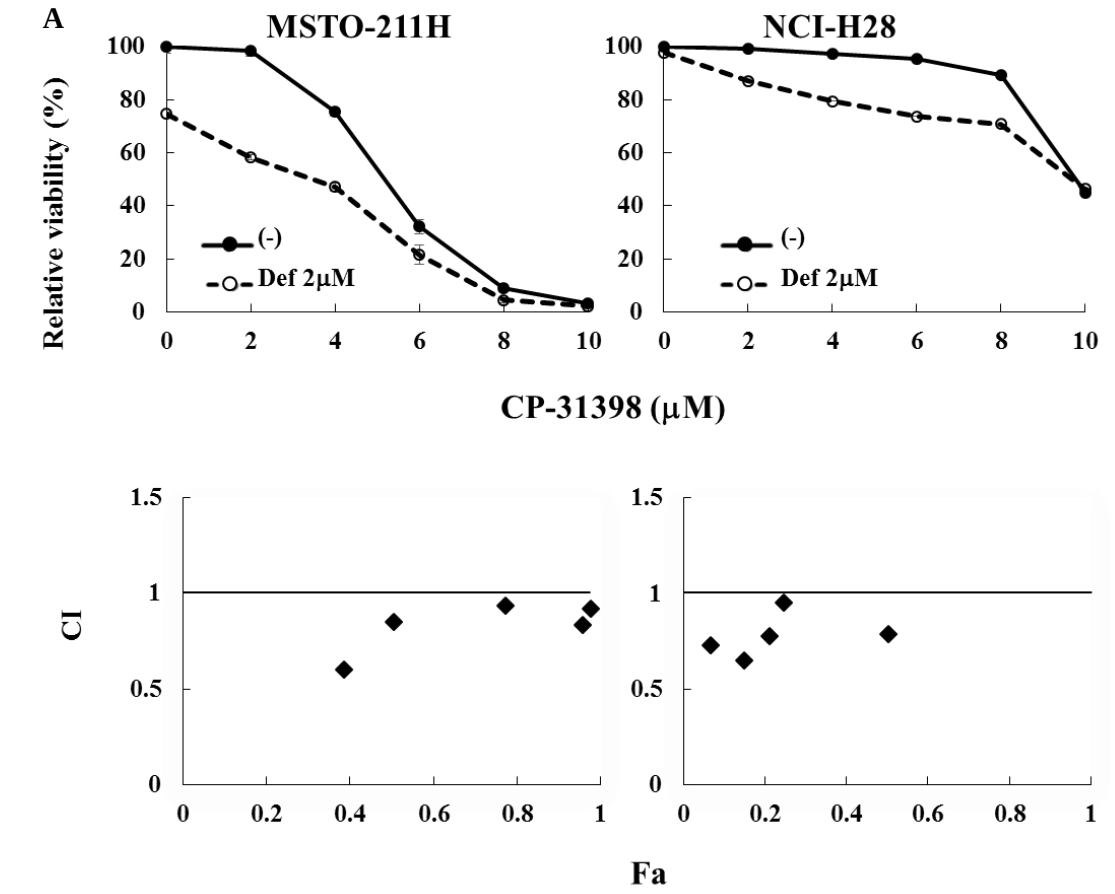
A
MSTO-211H
NCI-H28
Relative viability (%)
100
80
60
40
20
0
(-)
Def 2μM
0
2
4
6
8
10
CP-31398 (μM)
CI
1.5
1
0.5
0
0.2
0.4
0.6
0.8
Fa

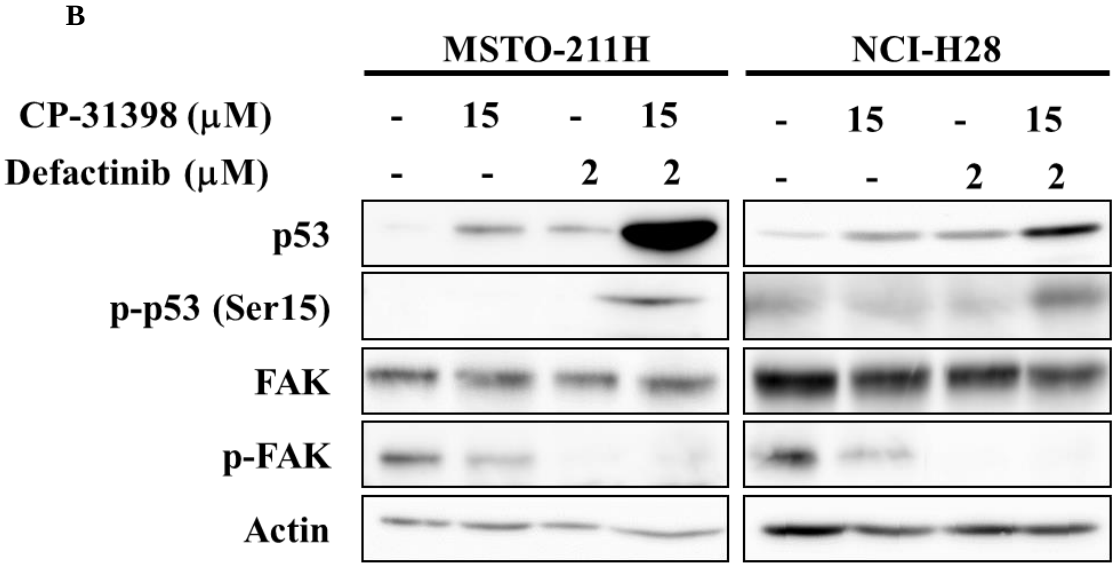
B
MSTO-211H
NCI-H28
CP-31398 (μM)
Defactinib (μM)
p53
p-p53 (Ser15)
FAK
p-FAK
Actin

Figure 6

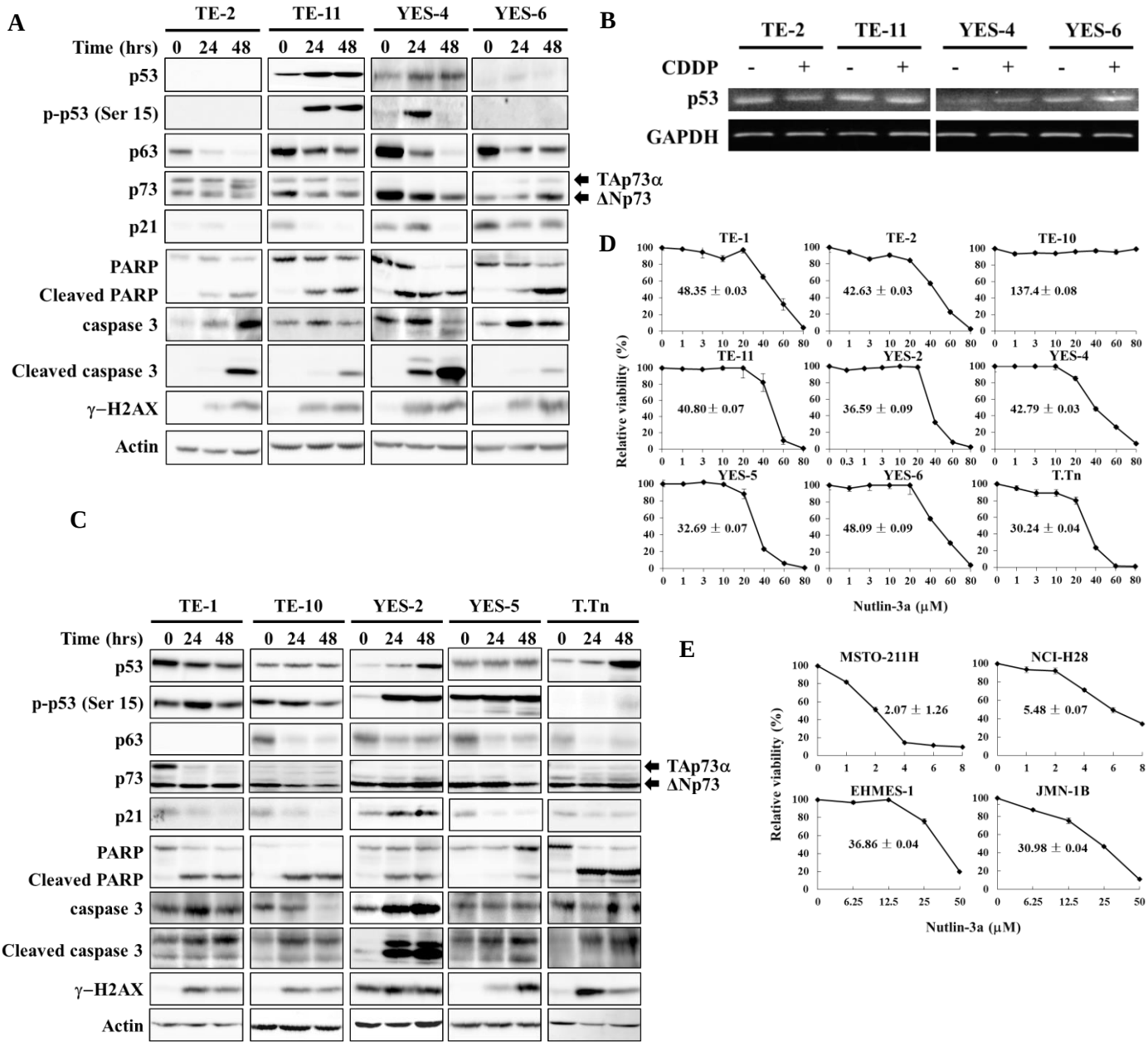
A
TE-2
TE-11
YES-4
YES-6
Time (hrs)
0 24 48
p53
p-p53 (Ser 15)
p63
p73
p21
PARP
Cleaved PARP
caspase 3
Cleaved caspase 3
γ−H2AX
Actin
TAp73α
ΔNp73
B
TE-2
TE-11
YES-4
YES-6
CDDP
- + - + - + - +
p53
GAPDH
C
TE-1
TE-10
YES-2
YES-5
T.Tn
Time (hrs)
0 24 48
p53
p-p53 (Ser 15)
p63
p73
p21
PARP
Cleaved PARP
caspase 3
Cleaved caspase 3
γ−H2AX
Actin
TAp73α
ΔNp73
D
TE-1
48.35 ± 0.03
TE-2
42.63 ± 0.03
TE-10
137.4± 0.08
TE-11
40.80± 0.07
YES-2
36.59 ± 0.09
YES-4
42.79 ± 0.03
YES-5
32.69 ± 0.07
YES-6
48.09 ± 0.09
T.Tn
30.24 ± 0.04
Relative viability (%)
Nutlin-3a (μM)
E
MSTO-211H
2.07 ± 1.26
NCI-H28
5.48 ± 0.07
EHMES-1
36.86 ± 0.04
JMN-1B
30.98 ± 0.04
Relative viability (%)
Nutlin-3a (μM)

Figure 7

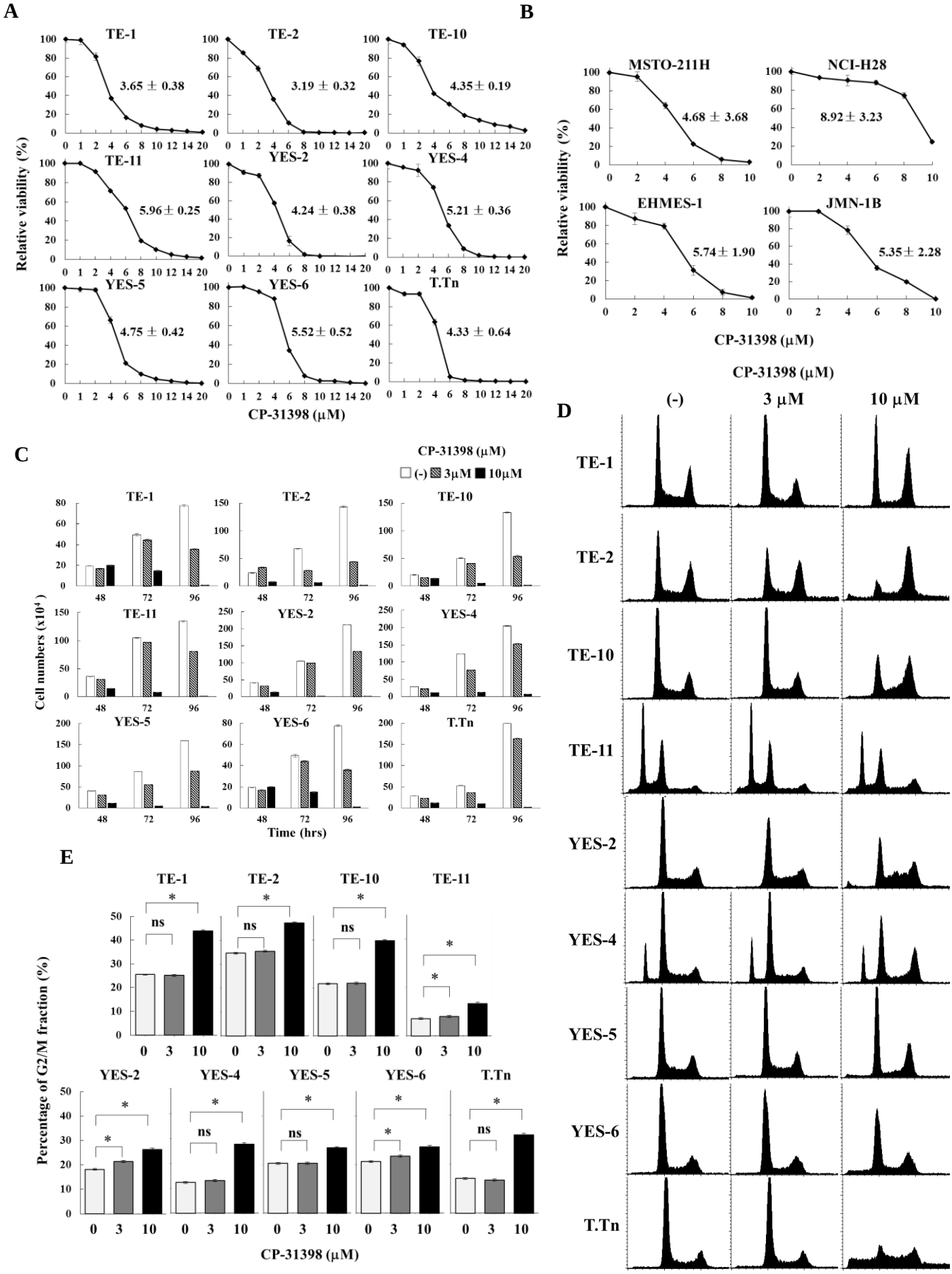
A
TE-1
3.65 ± 0.38
TE-2
3.19 ± 0.32
TE-10
4.35± 0.19
TE-11
5.96± 0.25
YES-2
4.24 ± 0.38
YES-4
5.21 ± 0.36
YES-5
4.75 ± 0.42
YES-6
5.52± 0.52
T.Tn
4.33 ± 0.64
Relative viability (%)
CP-31398 (μM)
B
MSTO-211H
4.68 ± 3.68
NCI-H28
8.92± 3.23
EHMES-1
5.74± 1.90
JMN-1B
5.35± 2.28
Relative viability (%)
CP-31398 (μM)
C
CP-31398 (μM)
(-) 3μM 10μM
Cell numbers (x10⁴)
Time (hrs)
D
(-)
3 μM
10 μM
E
Percentage of G2/M fraction (%)
ns
*
CP-31398 (μM)

Figure 8

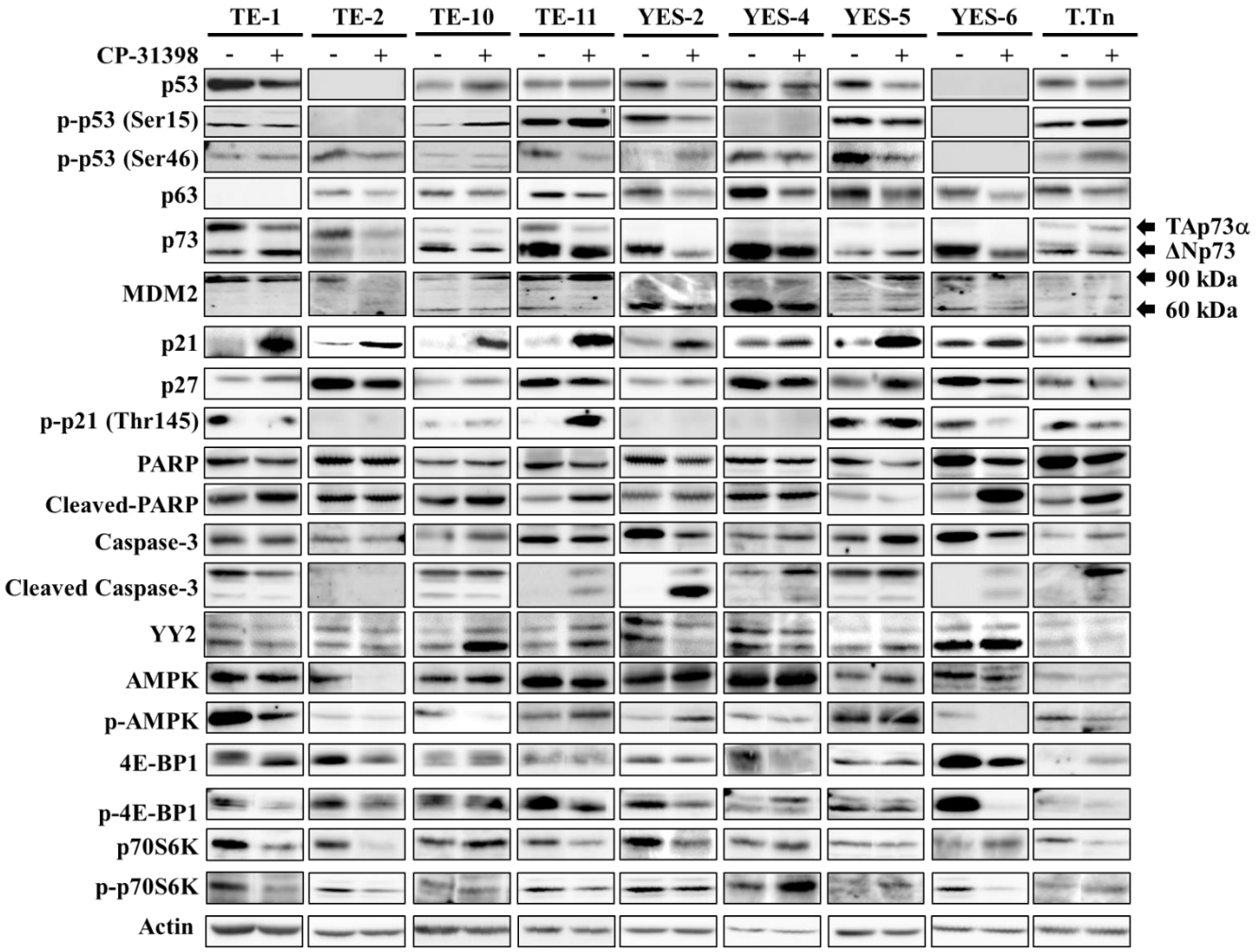
TE-1
TE-2
TE-10
TE-11
YES-2
YES-4
YES-5
YES-6
T.Tn
CP-31398
- + - + - + - + - + - + - + - + - +
p53
p-p53 (Ser15)
p-p53 (Ser46)
p63
p73
MDM2
p21
p27
p-p21 (Thr145)
PARP
Cleaved-PARP
Caspase-3
Cleaved Caspase-3
YY2
AMPK
p-AMPK
4E-BP1
p-4E-BP1
p70S6K
p-p70S6K
Actin
TAp73α
ΔNp73
90 kDa
60 kDa

Figure 9

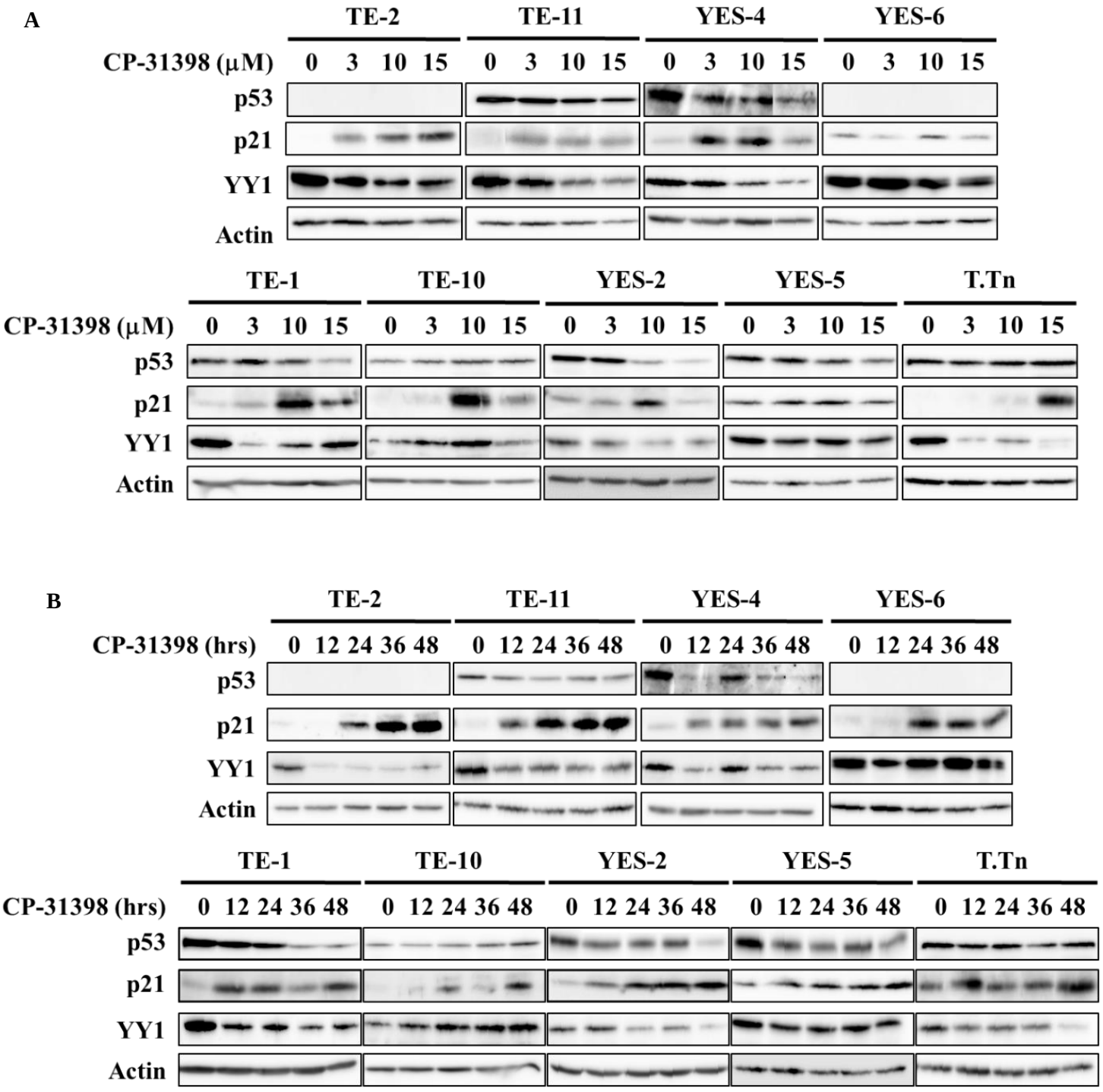
A
TE-2
TE-11
YES-4
YES-6
CP-31398 (μM)
0 3 10 15 0 3 10 15 0 3 10 15 0 3 10 15
p53
p21
YY1
Actin
TE-1
TE-10
YES-2
YES-5
T.Tn
CP-31398 (μM)
0 3 10 15 0 3 10 15 0 3 10 15 0 3 10 15 0 3 10 15
p53
p21
YY1
Actin
B
TE-2
TE-11
YES-4
YES-6
CP-31398 (hrs)
0 12 24 36 48 0 12 24 36 48 0 12 24 36 48 0 12 24 36 48
p53
p21
YY1
Actin
TE-1
TE-10
YES-2
YES-5
T.Tn
CP-31398 (hrs)
0 12 24 36 48 0 12 24 36 48 0 12 24 36 48 0 12 24 36 48 0 12 24 36 48
p53
p21
YY1
Actin

Figure 10

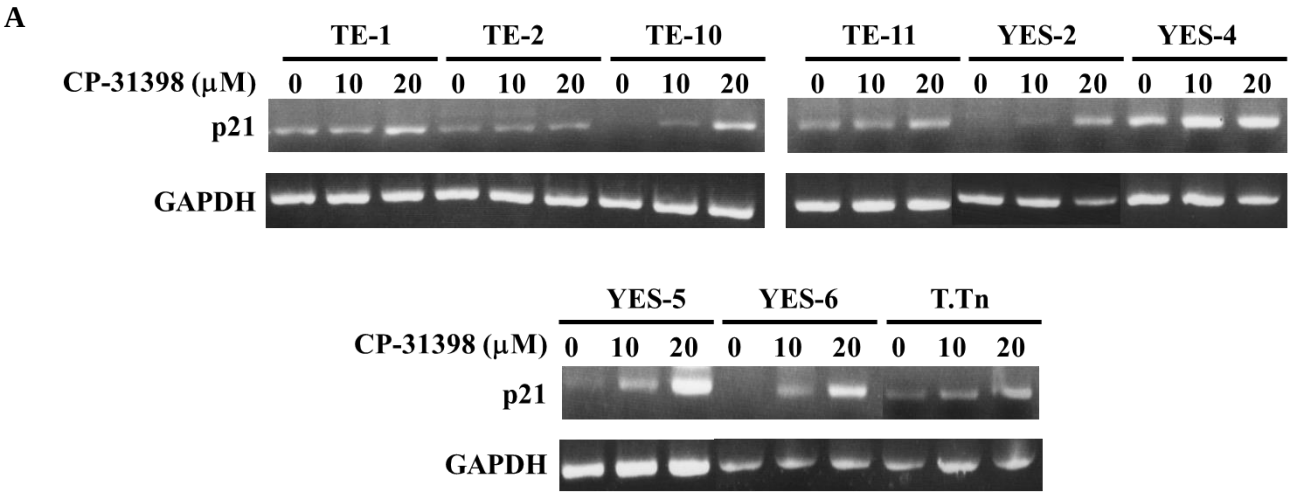
A
TE-1
TE-2
TE-10
TE-11
YES-2
YES-4
CP-31398 (μM)
0 10 20 0 10 20 0 10 20 0 10 20 0 10 20 0 10 20
p21
GAPDH
YES-5
YES-6
T.Tn
CP-31398 (μM)
0 10 20 0 10 20 0 10 20
p21
GAPDH

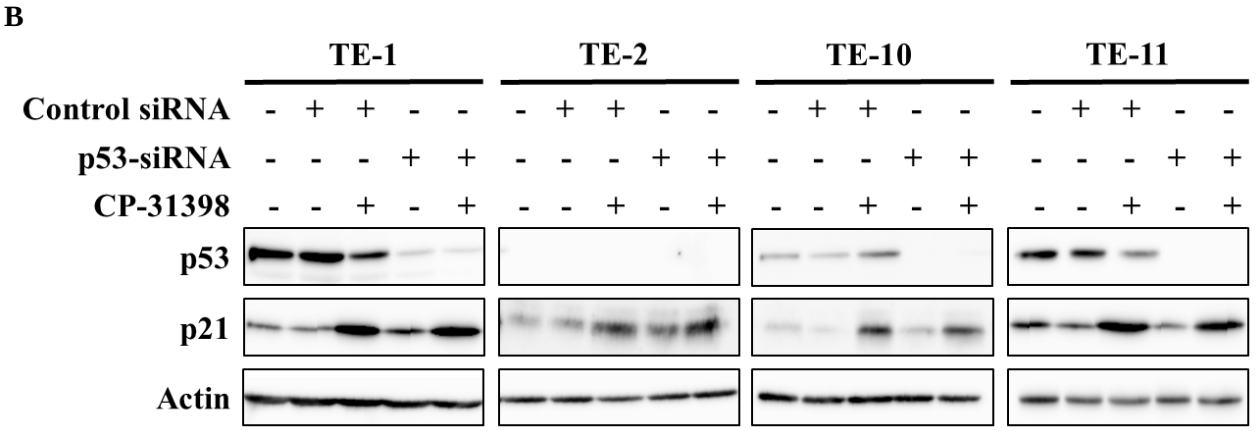
B
TE-1
TE-2
TE-10
TE-11
Control siRNA
p53-siRNA
CP-31398
p53
p21
Actin

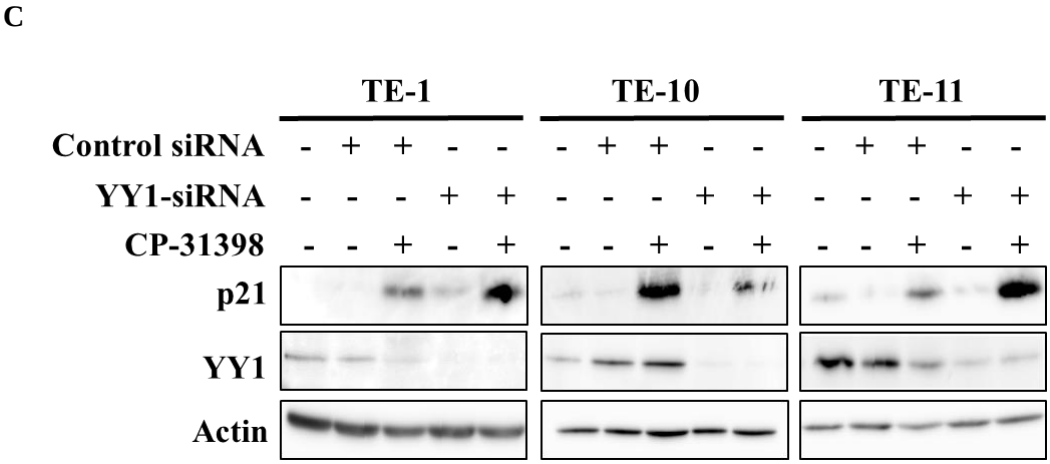
C
TE-1
TE-10
TE-11
Control siRNA
YY1-siRNA
CP-31398
p21
YY1
Actin

Figure 11

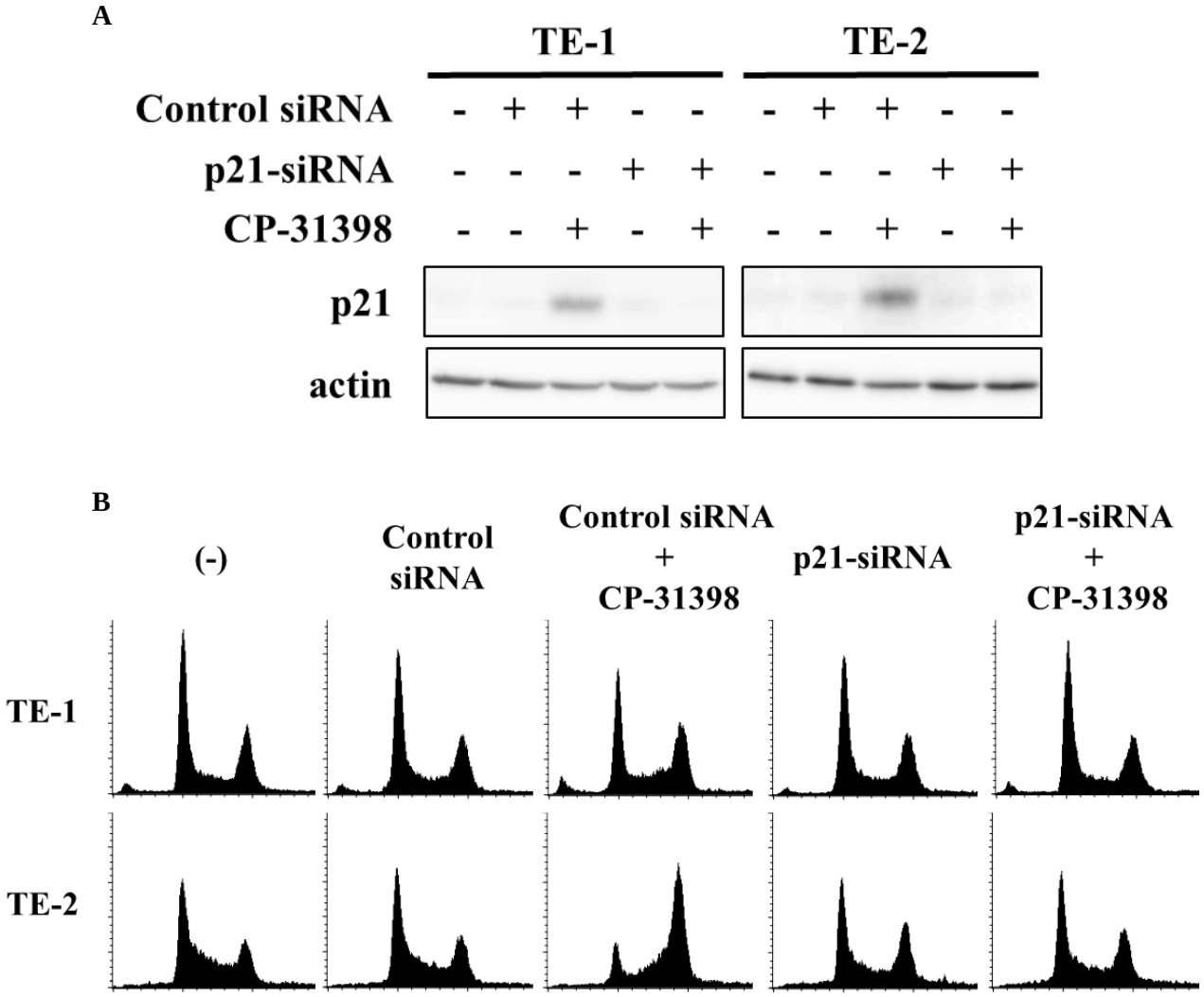
A
TE-1
TE-2
Control siRNA
p21-siRNA
CP-31398
p21
actin
B
(-)
Control siRNA
Control siRNA + CP-31398
p21-siRNA
p21-siRNA + CP-31398
TE-1
TE-2

Main article

Molecular Medicine

Submitted in October, 2018

Sub article

American Journal of Cancer Research, Vol 9, No 1

Published on 15th, January, 2019